File No. 13011L

Carolina Power & Light

Health Physics & Chemistry Section

Dosimetry Technical Report: 90-05

Brunswick TIP Incident Dose Calculations

November 30, 1990

Prepared By: S.A. Browne

Approved By: B. H. Webster

Brunswick TIP Incident Dose Calculations

Introduction

On July 5, 1990, Mr. Larry Dew was involved in a radiological incident which resulted in an unplanned exposure to his left hand while working on a job to install new transient in-core probes (TIPs) at the Brunswick Nuclear Plant. E&RC Experience Report Number 90-004 contains a complete description of the occurrence, its cause, and corrective actions. Since no monitoring devices were worn on the hand, it was necessary to calculate the dose based on the best information available, primarily obtained from interviews, records, and drawings. Originally, a total exposure to the hand of 10.6 rem was estimated by CP&L. However, Mr. Dew disagreed with the assumptions used and refused to sign the final Personnel Exposure Investigation report containing this dose. Subsequently, Mr. Dew filed a complaint with the Department of Labor which questioned the validity of the dose. As a result of the DOL allegations, the NRC requested additional information supporting the dose assignment. In response, CP&L reexamined the assumptions and methodology used in the dose calculations and concluded that the original exposure estimate was valid. This report summarizes the methodology and results of dose calculations.

General Assumptions

The shallow dose to the hand (7 mg/cm^2 tissue depth) represents the most limiting exposure case for the TIP incident. Since the exposed worker wore two pairs of rubber gloves, the dose was determined for both beta and gamma radiation at a depth of 99 mg/cm^2, which is the sum of the density thickness of the gloves and skin (See Attachment 1).

The dose calculations are based on two principal nuclides, Mn-56 and Al-28, which represented 95.6% of the total activity in the detector and 98.6% of the activity in the cable (see Attachment 2). The dose contribution other nuclides is small and is more than offset by conservative assumptions employed in the dose calculation.

The dose from the incident is calculated separately for exposure from the detector versus the drive cable because of differences in geometries, activities, and exposure times.

Many assumptions were made in performing the dose calculations, but the most critical ones concerned the length of time the TIP was in the core and the length of time different parts were touched. These times were determined based on interviews with participants in the incident and on reenactments, all of which are described more completely in Attachment 10. Because the actual times are unknown, upper and lower bound doses were calculated, in addition to a best estimate dose, in order to give an indication of the degree of uncertainty. The table below summarizes the time assumptions used in the dose calculations.

	Lower Bound	**Best Estimate**	Upper Bound
Time in Core	120 sec	**180 sec**	300 sec
Time Touching TIP	0	**0**	.5 sec
Time Touching Cable	3 sec	**4 sec**	4 sec

In addition to the above assumptions, the primary data used in the dose calculations were design information for the TIP (detector and cable materials and dimensions) and neutron activation analyses for various irradiation and decay times, both provided by Reuter-Stokes, Inc., the TIP manufacturer. Attachment 3 contains drawings and diagrams representing the detector and cable and Attachment 4 contains the results of neutron activation calculations.

Gamma Dose Calculations

The gamma dose was calculated using the computer code Microshield, a program for analyzing gamma radiation shielding (Ref. 4). The program input includes: geometry, source nuclides and activities, source and shield materials, dimensions of source and shields, and position at which dose rate is to be determined. The output is the dose rate at the specified point.

The basic geometry selected to model both the detector and the cable was a cylindrical source (side view) surrounded by cylindrical shields. For this geometry, Microshield calculates the exposure rate at a specified point using a point-kernel numerical integration technique. Three integration parameters determine how finely the source volume is divided for the numerical integration: radial, horizontal angle, and vertical angle. A value of 11 was selected, thus dividing the source into 11^3 differential volumes.

The dose for complex geometries can be approximated by breaking them into several simple geometries for which the dose can be calculated separately and then summed. In this case, the total gamma dose is the sum of three separate geometry and nuclide combinations.

1. Cable Containing Mn-56
The gamma dose from the cable was calculated only for Mn-56, since the activity of Al-28 was negligible. the activity was assumed to be uniformly distributed in a solid, cylindrical volume of iron, 18 inches long. Because of the small distance between the hand and the cable, the percent contribution to the dose from parts of the cable greater than 9 inches away is negligible. Attachment 5 shows the Microshield results.

2. TIP Insulators Containing Al-28
The Al-28 is contained in alumina (Al_2O_3) insulators inside the outer detector shell. The activity was assumed to be uniformly distributed in a solid, cylindrical volume representing the alumina surrounded by an iron shield representing the detector shell. Attachment 6 shows the Microshield results.

3. TIP Detector Shell Containing Mn-56
The Mn-56 is contained primarily in the stainless steel detector shell. The activity was assumed to be uniformly distributed in a hollow cylindrical volume representing the stainless steel shell. The dose from a hollow cylinder was obtained by calculating the dose from two solid cylinders of different diameters and subtracting the smaller from the larger. In this case, the diameters used were the inside and outside diameters of the detector shell. Attachment 7 shows the Microshield results.

The calculations for 120 second TIP irradiation times were done with Microshield and were adjusted using a spreadsheet program for different irradiation and exposure times. Attachment 8 contains a summary of the gamma dose calculations for each of the above three cases based on upper bound, lower bound and best estimate assumptions.

Beta Dose Calculations

The beta dose was calculated using equations which integrate the experimentally derived beta particle point source dose distribution function for several simple geometries (Ref. 2). The total beta dose is the sum of the beta dose for three different geometries and nuclide combinations:

1. Infinite, Plane Slab of Infinite Thickness
This geometry was assumed for the beta dose from Mn-56 in the cable. This is considered to be a reasonable, probably conservative, approximation for a hand wrapped around a long, cylindrical source (the cable) whose

radius exceeds the maximum beta particle range. The dose at a depth x outside an infinite, plane slab of infinite thickness is given by the following equation (Ref 2, p.722, Eq. 24):

$$D_\infty(x) = .5D_\beta\alpha\{c^2[3-e^{(1-\nu x/c)}-\nu x/c(2+\ln(c/\nu x))]+e^{(1-\nu x)}\}, \text{ rad}$$

$$[\ ] \equiv 0 \text{ for } x \geq c/\nu$$

Where:
$D_\beta = 2.13E_\beta\tau$, rad/hr
E_β = Average beta energy, MeV
τ = Activity concentration, μCi/g
$\alpha = [3c^2-(c^2-1)e]^{-1}$
c = 2 for $0.17<E_0<0.5$; 1.5 for $0.5\leq E_0<1.5$; 1 for $1.5\leq E_0<3$
$\nu = 18.6/(E_0-.036)^{1.37}$, cm^2/g
E_0 = Maximum beta energy, MeV
x = Depth in absorber outside slab, g/cm^2

2. Infinite, Plane Slab of Finite Thickness
This geometry was assumed for calculating the beta dose from Mn-56 in the outer detector shell of the TIP. It was chosen because the thickness of the detector shell is less than the maximum beta particle range. The dose at a point outside a infinite, plane slab of finite thickness is given by the following equation (Ref 2, p.725, Eq. 27):

$$D(x,h) = D(x,\infty)-D(x+h,\infty)$$

The terms on the right are given by equation 24.

3. Sphere Containing Uniformly Distributed Activity
This geometry was assumed for Al-28 beta dose calculation from the alumina insulators inside the outer shell of the detectors. The dose at a distance x from the center of a sphere of radius b is given by the following equation (Ref. 2, p.736, Eq. 38):

$$D_{sph}(x,b) = .5\alpha D_\beta[(\nu b+1)e^{-\nu b}+(\nu b-1)e^{\nu b}]e^{(1-\nu x)}/\nu x$$

For: $x \geq c/\nu+b$

Attachment 9 contains a summary of the beta dose calculations for each of the three geometries based on upper bound, lower bound and best estimate assumptions.

The dose contribution from bremsstrahlung radiation was considered negligible. The ratio, r, of energy loss from bremsstrahlung to that from collisions can be estimated by the following equation (Ref. 6, p. 175):

$$r \approx (TZ/700)$$

Where: T = beta particle energy
Z = atomic number of absorber

Assuming T equals the average energy of Mn-56 (.86 MeV) and Z equals the atomic number of iron (26), then r equals 3.1%. Since the bremsstrahlung radiation will deposit its energy over a range of absorber thickness, the dose contribution at the skin depth will be only a very small fraction of the 3.1%.

Total Dose

The total shallow dose to the hand from the TIP incident is simply the sum of the beta and gamma doses as summarized in the following table.

	Beta Dose (rad)	Gamma Dose (rem)	Total Dose (rem)
Lower Bound	4.623	0.698	5.321
Best Estimate	**9.228**	**1.392**	**10.620**
Upper Bound	36.385	7.687	44.072

Conservatisms

A number of conservative assumptions and approximations were used in performing the dose calculations. Several of those are discussed below, including estimates of the magnitude of the effect on dose calculations for some.

<u>Neutron Flux</u>
Reuter-Stokes used a flux of 5.0×10^{13} $n/cm^2/sec$ in the neutron activation calculations. It was later determined that the average neutron flux in the channel traversed by the TIP during the incident was 4.394×10^{13} $n/cm^2/sec$. This difference translates directly into a 14% conservatism in the calculated dose.

<u>Skin Depth</u>
NRC regulations require that the dose to the extremities be reported at a depth of 7 mg/cm^2, but the average epidermal thickness on palms of the hands is about 40 mg/cm^2 (Ref. 5, p.50). The beta dose at 40 mg/cm^2 is 18% less than at 7 mg/cm^2.

Geometry

In most cases the geometry was selected in a conservative manner. For example, the use of an infinite, plane slab for beta dose calculations will slightly over estimate the beta dose compared to a cylindrical geometry.

Electronic Equilibrium

For all gamma dose calculations electronic equilibrium was assumed to exist at the 7 mg/cm^2 depth. For high energy photons equilibrium will not be established at this depth, which will result in an over estimate of the gamma dose.

Decay Time

The decay time is the amount of time required to crank the TIP from the core to the TIP box. After leaving the core, the TIP must travel approximately 60 feet to reach the TIP box. At a normal speed of 1 foot per second, this would take about 60 seconds, however, during the incident the crank was difficult to turn and the speed was probably slower. Nevertheless, a decay time of only 30 seconds was assumed in the dose calculations, so that the activity assumed for the dose calculations is probably conservatively high. The effect is small for Mn-56 which has a half-life of 2.6 hours, but is significant for Al-28 which has a half-life of 2.24 minutes.

Independent Evaluation of Dose Calculations

Mr. Robert E. Alexander, a health physics consultant, was engaged by CP&L to perform an independent evaluation of the dose calculations for this incident. His report, reproduced in Attachment 11, confirms the validity and conservatism of the CP&L dose calculations. The beta dose, which is the largest component, was recalculated using a Monte Carlo simulation code by Dr. Thomas R. Mackie of the University of Wisconsin. The results are in excellent agreement (within 7 percent) with the CP&L dose calculation performed using equations published by Hine and Brownell in Radiation Dosimetry.

Conclusion

The original estimate of the dose to the left hand of Mr. Larry Dew was 10.6 rem. After a thorough reexamination of all assumptions and calculation methods, this is still considered to be a valid and probably conservative estimate of the dose received during the TIP incident. Therefore, no changes are recommended to the previously assigned dose to Mr. Dew.

References

1. Radiation Health Handbook, U.S. Department of Health, Education, and Welfare, Public Health Service, January 1970.

2. Radiation Dosimetry, G. J. Hine and G. L. Brownell, Eds., Academic Press, New York, 1956, Chapter 16.

3. Principles of Radiation Protection, K. A. Morgan and J. E. Turner, Eds., John Wiley & Sons, New York, 1967, Chapter 8.

4. Microshield 3 Manual, Grove Engineering, Inc., Washington Grove, MD, 1988.

5. ICRP Publication 23: Report of the Task Group on Reference Man, Committee 2 of the ICRP, Pergamon Press, New York, 1975.

6. Radiation Dosimetry, 2nd Edition, Volume I: Fundamentals, F. H. Attix and W. C. Roesch, Eds., Academic Press, New York, 1968.

Attachment 1

Depth at Which Dose Calculated

The dose was calculated at a depth equivalent to the thickness of two pairs of rubber gloves plus the thickness of skin. The glove thickness was determined by weighing a sample of glove material of known area.

Glove sample area = 25 cm^2

Glove sample weight = 1.15 g

Single glove thickness = .046 g/cm^2

Double glove thickness = .092 g/cm^2

Skin thickness = .007 g/cm^2

Total depth = .092 + .007 = .099 g/cm^2

Attachment 2

Principal Nuclide Decay and Emission Data

Al-28

Atomic number	: 13
Atomic weight	: 28
Half life	: 2.24 minutes

============ Betas: ============

	probability per decay	maximum (MEV)	average (MEV)
1	1.000000	2.864200	1.242300

======= Gammas & X-rays: =======

	probability per decay	energy (MEV)
1	1.000000	1.778900

Mn-56

Atomic number	: 25
Atomic weight	: 56
Half life	: 2.5785 hours

============ Betas: ============

	probability per decay	maximum (MEV)	average (MEV)
1	.011600	.325630	.099100
2	.146000	.735530	.255200
3	.278000	1.037900	.381900
4	.562000	2.848600	1.216700
5	.001189	.987800	.373140

======= Gammas & X-rays: =======

	probability per decay	energy (MEV)
1	.988700	.846750
2	.271890	1.810700
3	.143360	2.113100
4	.009887	2.522900
5	.006525	2.657500
6	.003065	2.959800
7	.001681	3.369600
8	.001626	1.351400

Attachment 3

TIP Drawings

REUTER-STOKES

FACSIMILE TRANSMITTAL

Twinsburg, OH
216 425-3755 Fax 216 425-4045

DATE: 23 OCT 90

PAGE: 1 of ______

CLASSIFICATION:

- [X] Information
- [ ] Action

DISTRIBUTION

TO: STEVE BROWN
CP+L

FAX #: 919 546 4361

FROM: TIM KNISS
G.E. REUTER-STOKES

SENT BY: ______

SUBJECT: INTERNAL COMPONENTS IN GAMMA TIP SENSOR

MESSAGE:

STEVE,

I HOPE THERE IS SUFFICIENT DETAIL ON THESE DRAWINGS TO HELP YOU WITH YOUR CALCULATIONS.

PART 10 IS THE DETECTOR HOUSING, 1.980" LONG AND .211" O.D., .1704" I.D., 304L SS.

PIECES 8, 11, AND 15 ARE THE ALUMINUM OXIDE INSULATORS INSIDE THE DETECTOR.

4-56
NOTE 7

GE/REUTER - STOKES PROPRIETARY INFORMATION

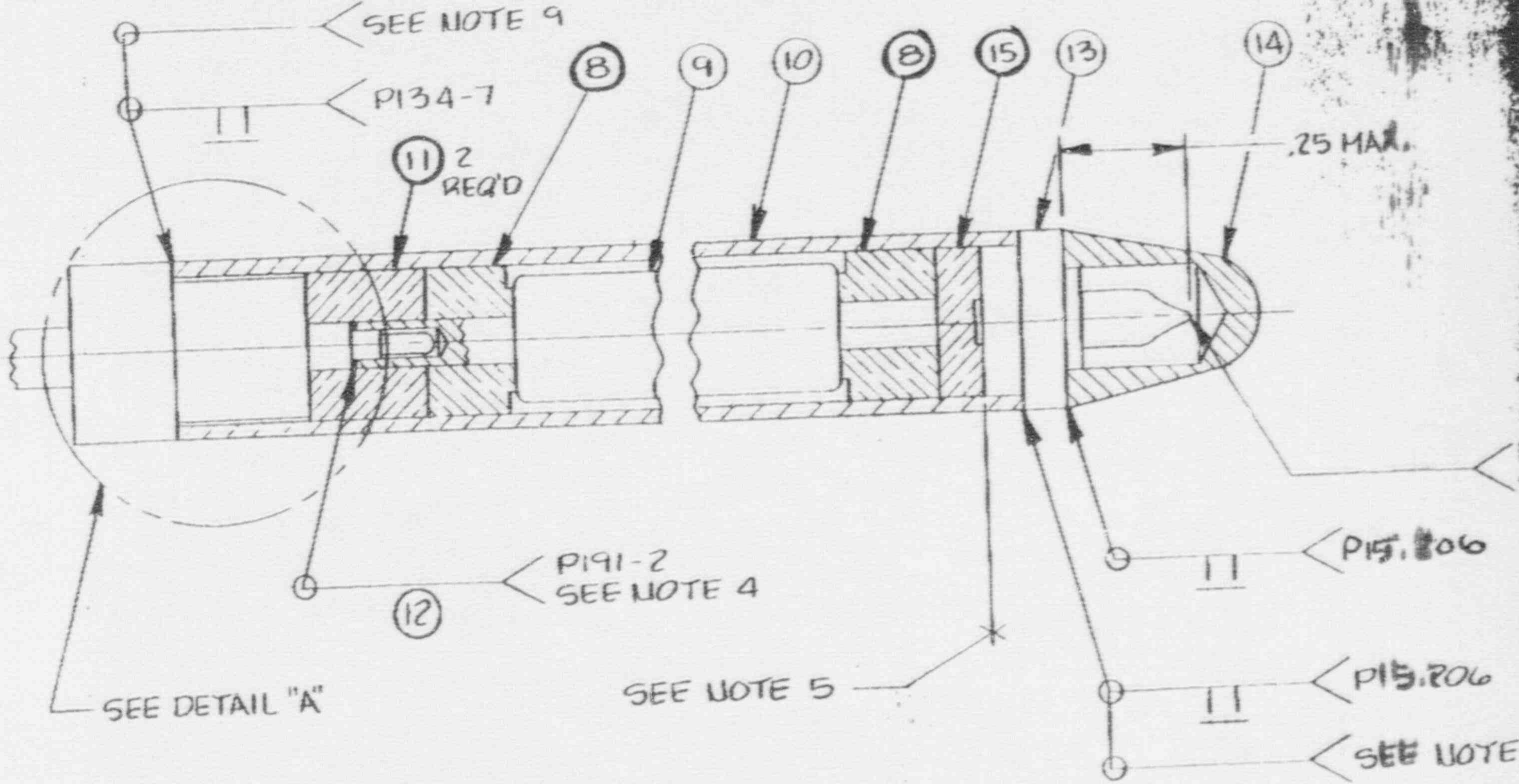

SECTION B-B
ENLARGED

GE/REUTER - STOKES PROPRIETARY INFORMATION

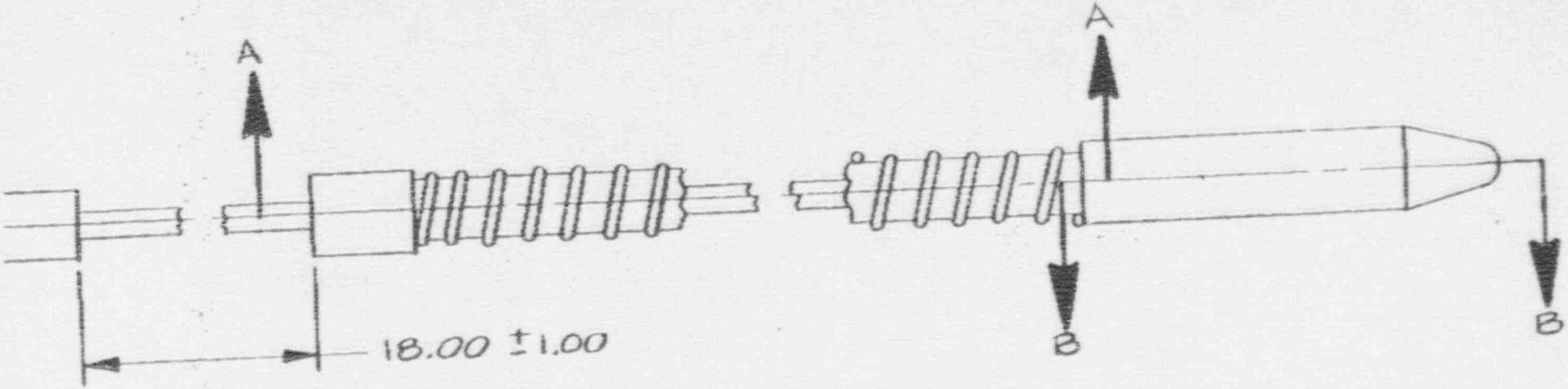

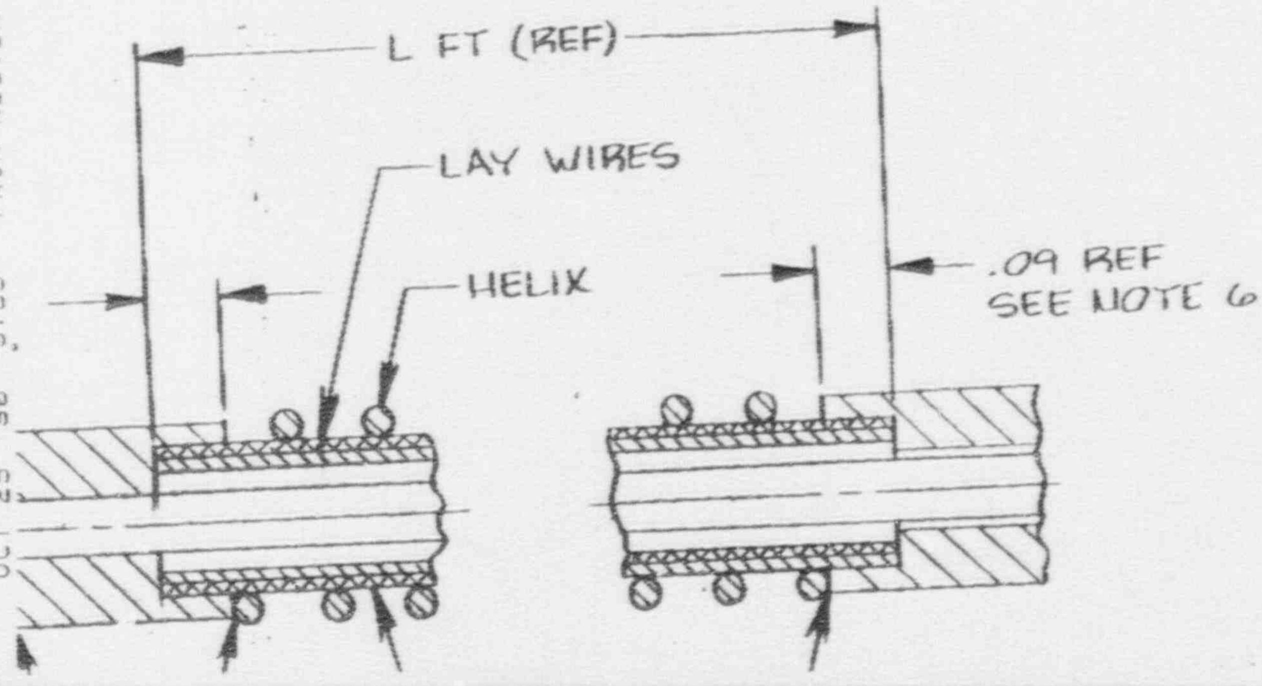

Attachment 4

Neutron Activation Calculations

KIT: 30

CABLE (9')

NEUTRON ACTIVATION CALCULATION — 07/17/90 09:18 AM

SAMPLE NAME: GAMMA TIP CABLE

PARENT Element	Mass	DAUGHTER Isotope	Curies	ACTIVITY Isotope	Curies	IRRADIATION CONDITIONS	
Na	0.00	Na24	0.000	Fe59	0.000	Flux:	5.0E+13
Mg	5.17	Mg27	0.060	Co58	0.000	Time:	180
Al	0.00	Al28	0.007	Co60	0.000		
Ti	0.00	Sc46	0.000	Ni57	0.000	Moderator Temp	
Cr	8.60	Sc47	0.000	Ni65	0.000	(Deg C):	285
Mn	3.09	Sc48	0.000	Cu64	0.000		
Fe	261.00	Ti45	0.000	Cu66	0.000	Fast Flux	
Co	0.05	Ti51	0.000	Mo93	0.000	Factor:	0.8
Ni	0.00	Cr51	0.003	Mo99	0.000		
Cu	0.00	Mn54	0.000	Mo101	0.000	Cooling Down	
Mo	0.00	Mn56	5.241	Ta182	0.000	Time:	30
Ta	0.00		TOTAL:		5.312	Mode:	c

DECAY OF ACTIVITY

17-Jul-90 09:18 AM OnLine CapsNum

KIT: 60

NEUTRON ACTIVATION CALCULATION — 07/17/90 09:19 AM

SAMPLE NAME: GAMMA TIP CABLE

PARENT Element	Mass	DAUGHTER Isotope	Curies	ACTIVITY Isotope	Curies	IRRADIATION CONDITIONS	
Na	0.00	Na24	0.000	Fe59	0.000	Flux:	5.0E+13
Mg	5.17	Mg27	0.058	Co58	0.000	Time:	180
Al	0.00	Al28	0.006	Co60	0.000		
Ti	0.00	Sc46	0.000	Ni57	0.000	Moderator Temp	
Cr	8.60	Sc47	0.000	Ni65	0.000	(Deg C):	285
Mn	3.08	Sc48	0.000	Cu64	0.000		
Fe	261.00	Ti45	0.000	Cu66	0.000	Fast Flux	
Co	0.05	Ti51	0.000	Mo93	0.000	Factor:	0.8
Ni	0.00	Cr51	0.003	Mo99	0.000		
Cu	0.00	Mn54	0.000	Mo101	0.000	Cooling Down	
Mo	0.00	Mn56	5.229	Ta182	0.000	Time:	60
Ta	0.00		TOTAL:		5.297	Mode:	c

DECAY OF ACTIVITY

17-Jul-90 09:19 AM OnLine CapsNum

GAMMA TIP

A1:

NEUTRON ACTIVATION CALCULATION — 07/17/90 09:03 AM

SAMPLE NAME:

PARENT Element	Mass	DAUGHTER Isotope	Curies	ACTIVITY Isotope	Curies	IRRADIATION CONDITIONS	
Na	0.00	Na24	0.000	Fe59	0.000	Flux:	5.0E+13
Mg	0.01	Mg27	0.000	Co58	0.000	Time:	180
Al	0.44	Al28	1.017	Co60	0.000		
Ti	0.65	Sc46	0.000	Ni57	0.000	Moderator Temp	
Cr	0.93	Sc47	0.000	Ni65	0.001	(Deg C):	285
Mn	0.10	Sc48	0.000	Cu64	0.001		
Fe	3.51	Ti45	0.000	Cu66	0.038	Fast Flux	
Co	0.05	Ti51	0.015	Mo93	0.000	Factor:	0.8
Ni	0.47	Cr51	0.000	Mo99	0.000		
Cu	0.02	Mn54	0.000	Mo101	0.000	Cooling Down	
Mo	0.00	Mn56	0.169	Ta182	0.000	Time:	30
Ta	0.00		TOTAL:		1.241	Mode:	c

DECAY OF ACTIVITY

17-Jul-90 09:05 AM OnLine Num

K17: 60

NEUTRON ACTIVATION CALCULATION — 07/17/90 09:06 AM

SAMPLE NAME:

PARENT Element	Mass	DAUGHTER Isotope	Curies	ACTIVITY Isotope	Curies	IRRADIATION CONDITIONS	
Na	0.00	Na24	0.000	Fe59	0.000	Flux:	5.0E+13
Mg	0.01	Mg27	0.000	Co58	0.000	Time:	180
Al	0.44	Al28	0.876	Co60	0.000		
Ti	0.65	Sc46	0.000	Ni57	0.000	Moderator Temp	
Cr	0.93	Sc47	0.000	Ni65	0.001	(Deg C):	285
Mn	0.10	Sc48	0.000	Cu64	0.001		
Fe	3.51	Ti45	0.000	Cu66	0.035	Fast Flux	
Co	0.05	Ti51	0.014	Mo93	0.000	Factor:	0.8
Ni	0.47	Cr51	0.000	Mo99	0.000		
Cu	0.02	Mn54	0.000	Mo101	0.000	Cooling Down	
Mo	0.00	Mn56	0.169	Ta182	0.000	Time:	60
Ta	0.00		TOTAL:		1.096	Mode:	c

DECAY OF ACTIVITY

17-Jul-90 09:06 AM OnLine Num

Attachment 5

Microshield Results for Cable Containing Mn-56

Microshield 3.13

(Carolina Power & Light - #059)

Page : 1
File : CABLE120.MSH
Run date: November 27, 1990
Run time: 8:45 a.m.

File Ref: ______
Date: __/__/__
By: ______
Checked: ______

CASE: Cable - Manganese 56 - 120 sec Irradiation

GEOMETRY 7: Cylindrical source from side - cylindrical shields

Distance to detector..........................	X	0.422	cm.
Source length..................................	L	45.720	"
Dose point height from base..................	Y	22.860	"
Source cylinder radius........................	T1	0.323	"
Thickness of second shield...................	T2	0.099	"
Microshield inserted air gap.................	air	0.	"

Source Volume: 14.9462 cubic centimeters

MATERIAL DENSITIES (g/cc):

Material	Source	Shield 2	Air gap
Air			.001220
Aluminum			
Carbon			
Concrete			
Hydrogen			
Iron	7.860		
Lead			
Lithium			
Nickel			
Tin			
Titanium			
Tungsten			
Urania			
Uranium			
Water		1.0	
Zirconium			

CASE: Cable - Manganese 56 - 120 sec Irradiation

BUILDUP FACTOR: based on TAYLOR method.
Using the characteristics of the materials in shield 1.

INTEGRATION PARAMETERS:

Number of lateral angle segments (Ntheta).....	11
Number of azimuthal angle segments (Npsi).....	11
Number of radial segments (Nradius)..........	11

SOURCE NUCLIDES:

Nuclide	Curies	Nuclide	Curies	Nuclide	Curies
Al-28	0.0000e+00	Cr-51	0.0000e+00	Mg-27	0.0000e+00
Mn-56	5.8360e-01				

RESULTS:

Group #	Energy (MeV)	Activity (photons/sec)	Dose point flux MeV/(sq cm)/sec	Dose rate (mr/hr)
1	3.3672	3.629e+07	1.521e+06	2.073e+03
2	2.9609	6.618e+07	2.440e+06	3.505e+03
3	2.6641	1.409e+08	4.688e+06	6.971e+03
4	2.5234	2.135e+08	6.732e+06	1.020e+04
5	2.1172	3.096e+09	8.226e+07	1.312e+05
6	1.8047	5.871e+09	1.332e+08	2.244e+05
7	1.3516	3.512e+07	5.977e+05	1.076e+03
8	.8516	2.135e+10	2.301e+08	4.578e+05
9				
10				
11				
12				
13				
14				
15				
16				
17				
18				
19				
20				
TOTALS:		3.081e+10	4.616e+08	8.371e+05

Attachment 6

Microshield Results for Insulators in TIP Containing Al-28

Microshield 3.11

(Carolina Power & Light - #059)

Page : 1
File : TIPAL120.MSH
Run date: November 27, 1990
Run time: 8:47 a.m.

File Ref: ________
Date: __/__/__
By: ________
Checked: ________

CASE: Holding TIP - Aluminum-28 - 120 sec. Irradiation

GEOMETRY 7: Cylindri' l source from side - cylindrical shields

Distance to detector...........................	X	0.367	cm.
Source length..................................	L	2.540	"
Dose point height fro' base....................	Y	1.270	"
Source cylinder rad'us.........................	T1	0.216	"
Thickness of second shield.....................	T2	0.052	"
Thickness of third shield......................	T3	0.099	"
Microshield inserted air gap...................	air	0.	"

Source Volume: .373706 cubic centimeters

MATERIAL DENSITIES (g/cc):

Material	Source	Shield 2	Shield 3	Air gap
Air				.001220
Aluminum				
Carbon				
Concrete				
Hydrogen				
Iron		7.860		
Lead				
Lithium				
Nickel				
Tin				
Titanium				
Tungsten				
Urania				
Uranium				
Water			1.0	
Zirconium				
AlO				
Alumina	3.970			

BUILDUP FACTOR: based on TAYLOR method.
Using the characteristics of the materials in shield 3.

INTEGRATION PARAMETERS:

Number of lateral angle segments (Ntheta).....	11
Number of azimuthal angle segments (Npsi).....	11
Number of radial segments (Nradius)...........	11

SOURCE NUCLIDES:

Al-28: 7.7700e-01 curies

RESULTS:

Group #	Energy (MeV)	Activity (photons/sec)	Dose point flux MeV/(sq cm)/sec	Dose rate (mr/hr)
1	1.7734	2.875e+10	1.188e+10	2.010e+07
2				
3				
4				
5				
6				
7				
8				
9				
10				
11				
12				
13				
14				
15				
16				
17				
18				
19				
20				
	TOTALS:	2.875e+10	1.188e+10	2.010e+07

Attachment 7

Microshield Results for TIP Outer Shell Containing Mn-56

Microshield 3.11

(Carolina Power & Light - #059)

Page : 1
File : TIPOUTMN.MSH
Run date: November 27, 1990
Run time: 8:54 a.m.

File Ref:
Date: ___/___/___
By: ________
Checked: ________

CASE: TIP - Outer Cylinder - Manganese 56 - 120 sec. Irradiation

GEOMETRY 7: Cylindrical source from side - cylindrical shields

Distance to detector........................	X	0.367	cm.
Source length................................	L	5.080	"
Dose point height from base..................	Y	2.540	"
Source cylinder radius.......................	T1	0.268	"
Thickness of second shield...................	T2	0.099	"
Microshield inserted air gap.................	air	0.	"

Source Volume: 1.146 cubic centimeters

MATERIAL DENSITIES (g/cc):

Material	Source	Shield 2	Air gap
Air			.001220
Aluminum			
Carbon			
Concrete			
Hydrogen			
Iron	7.860		
Lead			
Lithium			
Nickel			
Tin			
Titanium			
Tungsten			
Urania			
Uranium			
Water		1.0	
Zirconium			

BUILDUP FACTOR: based on TAYLOR method.
Using the characteristics of the materials in shield 1.

INTEGRATION PARAMETERS:

Number of lateral angle segments (Ntheta).....	11
Number of azimuthal angle segments (Npsi).....	11
Number of radial segments (Nradius)...........	11

SOURCE NUCLIDES:

Mn-56: 3.2400e-01 curies

RESULTS:

Group #	Energy (MeV)	Activity (photons/sec)	Dose point flux MeV/(sq cm)/sec	Dose rate (mr/hr)
1	3.3672	2.015e+07	8.455e+06	1.152e+04
2	2.9609	3.674e+07	1.356e+07	1.948e+04
3	2.6641	7.823e+07	2.605e+07	3.875e+04
4	2.5234	1.185e+08	3.742e+07	5.670e+04
5	2.1172	1.719e+09	4.571e+08	7.290e+05
6	1.8047	3.259e+09	7.407e+08	1.247e+06
7	1.3516	1.950e+07	3.326e+06	5.988e+03
8	.8516	1.185e+10	1.285e+09	2.556e+06
9				
10				
11				
12				
13				
14				
15				
16				
17				
18				
19				
20				
	TOTALS:	1.710e+10	2.571e+09	4.664e+06

?±?

Microshield 3.11

(Carolina Power & Light - #059)

Page : 1
File : TIPINMN.MSH
Run date: November 27, 1990
Run time: 9:01 a.m.

File Ref:
Date: __/__/__
By:
Checked:

CASE: TIP - Inner Cylinder - Manganese 56 - 120 sec. Irradiation

GEOMETRY 7: Cylindrical source from side - cylindrical shields

Distance to detector..........................	X	0.367	cm.
Source length..................................	L	5.080	"
Dose point height from base...................	Y	2.540	"
Source cylinder radius........................	T1	0.216	"
Thickness of second shield....................	T2	0.099	"
Microshield inserted air gap..................	air	0.052	"

Source Volume: .747412 cubic centimeters

MATERIAL DENSITIES (g/cc):

Material	Source	Shield 2	Air gap
Air			.001220
Aluminum			
Carbon			
Concrete			
Hydrogen			
Iron	7.860		
Lead			
Lithium			
Nickel			
Tin			
Titanium			
Tungsten			
Urania			
Uranium			
Water		1.0	
Zirconium			

BUILDUP FACTOR: based on TAYLOR method.
Using the characteristics of the materials in shield 1.

INTEGRATION PARAMETERS:

Number of lateral angle segments (Ntheta)..... 11
Number of azimuthal angle segments (Npsi)..... 11
Number of radial segments (Nradius)........... 11

SOURCE NUCLIDES:

Mn-56: 2.1100e-01 curies

RESULTS:

Group #	Energy (MeV)	Activity (photons/sec)	Dose point flux MeV/(sq cm)/sec	Dose rate (mr/hr)
1	3.3672	1.312e+07	5.378e+06	7.328e+03
2	2.9609	2.393e+07	8.627e+06	1.239e+04
3	2.6641	5.094e+07	1.657e+07	2.464e+04
4	2.5234	7.719e+07	2.379e+07	3.605e+04
5	2.1172	1.119e+09	2.905e+08	4.633e+05
6	1.8047	2.123e+09	4.706e+08	7.925e+05
7	1.3516	1.270e+07	2.115e+06	3.805e+03
8	.8516	7.719e+09	8.164e+08	1.624e+06
9				
10				
11				
12				
13				
14				
15				
16				
17				
18				
19				
20				
TOTALS:		1.114e+10	1.634e+09	2.964e+06

Attachment 8

Gamma Dose Summary for TIP Incident

Gamma Dose Summary for the TIP Incident
(All calculations performed using Microshield, Rev. 3.11)

Object	Nuclides	Irr. Time (sec)	Activity (Ci)	Dose Rate (mR/h)	Dose Rate (R/s)	Exp. Time (sec)	Dose (R)
Cable	Mn-56	120	0.584	837100	0.233	3.0	0.698
TIP	Mn-56	120	0.113	1720000	0.478	0.0	0.000
TIP	Al-28	120	0.777	20100000	5.583	0.0	0.000
						Total:	0.698

Object	Nuclides	Irr. Time (sec)	Activity (Ci)	Dose Rate (mR/h)	Dose Rate (R/s)	Exp. Time (sec)	Dose (R)
Cable	Mn-56	180	0.874	1252925	0.348	4.0	1.392
TIP	Mn-56	180	0.169	2572389	0.715	0.0	0.000
TIP	Al-28	180	1.017	26308494	7.308	0.0	0.000
						Total:	1.392

Object	Nuclides	Irr. Time (sec)	Activity (Ci)	Dose Rate (mR/h)	Dose Rate (R/s)	Exp. Time (sec)	Dose (R)
Cable	Mn-56	300	1.449	2078406	0.577	4.0	2.309
TIP	Mn-56	300	0.280	4261947	1.184	0.5	0.592
TIP	Al-28	300	1.332	34457143	9.571	0.5	4.786
						Total:	7.687

Attachment 9

Beta Dose Summary for TIP Incident

Beta Dose Summary for TIP Incident

Object	Nuclide	Irr. Time (sec)	Exp. Time (sec)	Dose Rate (rad/s)	Dose (rad)
Cable	Mn-56	120	3	1.541	4.623
TIP	Mn-56	120	0	2.406	0
TIP	Al-28	120	0	21.109	0
				Total:	4.623

Object	Nuclide	Irr. Time (sec)	Exp. Time (sec)	Dose Rate (rad/s)	Dose (rad)
Cable	Mn-56	180	4	2.307	9.228
TIP	Mn-56	180	0	2.406	0
TIP	Al-28	180	0	21.109	0
				Total:	9.228

Object	Nuclide	Irr. Time (sec)	Exp. Time (sec)	Dose Rate (rad/s)	Dose (rad)
Cable	Mn-56	300	4	3.827	15.308
TIP	Mn-56	300	0.5	5.968	2.984
TIP	Al-28	300	0.5	36.186	18.093
				Total:	36.385

Attachment 10

As a result of the Department of Labor proceeding brought by Mr. Larry Dew against CP&L and CDI Corporation, CP&L conducted an investigation into the allegations. Part of this investigation centered around the radiation dose assigned to Mr. Dew.

The investigation of the dose assignment was divided into two parts: 1) the assumptions, and 2) the dose calculation methodology. The investigation regarding the assumptions was conducted by Mr. Mike McGarry and Mr. Don Meindertsma, counsel from the law firm of Winston and Strawn, Washington, DC, and, assisting at their direction, Mr. B. H. Webster, Manager of Corporate Health Physics for CP&L. The second part of the investigation that looked at the methodology for the dose calculation was conducted at the direction of legal counsel by Mr. Steve Browne and Mr. Jay Terry, technical representatives of CP&L, with assistance from an outside consultant, Mr. Robert Alexander.

In looking at the assumptions the investigation team sought the answers to four questions:

1. How long was the TIP in the core?

2. How far back from the detector did Mr. Dew grab the cable?

3. Did Mr. Dew actually touch the TIP detector?

4. How long was Mr. Dew's hand in contact with the TIP cable/detector?

In order to obtain answers to these questions, everyone involved or who might have knowledge of the incident was questioned, except Mr. Dew, who was not available. In all this included about 26 people, some of whom were questioned more than one time. In answering these questions, the investigation team determined the most probable scenario and also determined the upper and lower bounds for the assumptions as summarized in the table below.

SUMMARY OF ASSUMPTIONS			
	Lower Bound	Most Probable	Upper Bound
Time detector in core	2 min.	3 min.	5 min.
Distance from hand to detector	7 inches	7 inches	7 inches
Hand contact with detector	0 sec.	0 sec.	0.5 sec.
Hand in contact with cable	3 sec.	4 sec.	4 sec.

The findings of the investigation team with respect to the four questions and the conclusions regarding the assumptions used in the dose calculations are discussed below.

1. *How Long was the TIP in the core?*

   People who were involved in the work associated with this incident and others who were familiar with this type of work were questioned. Those people most familiar with the TIP operation stated that the TIP could not have been in the core more than two to three minutes. Only one person indicated that it could have been in the core as much as five minutes.

   Also, the dose recorded on the whole body badge substantiates the assumption that the TIP was not in the core for a much longer period. If the TIP had been in the core for eight to twelve minutes as alleged by Mr. Dew, our calculations show his whole body badge would have shown between 1,000 and 1,200 mrem. In fact, the whole body badge registered 405, which is consistent with the TIP being in the core for two to three minutes. For these reasons the investigation team believes that the best estimate of the time the detector was in the core was three minutes, with a range of two to five minutes.

2. *How far back from the detector did Mr. Dew grab the cable?*

   Following the incident, witnesses recalled that Mr. Dew repeatedly stated that he grabbed the cable about 12" from the detector and re-inserted it in the tube. However, in reenactment of the incident, Mr. Dew grabbed the cable as close as 7" from the detector. Consequently, for all cases, it was assumed that Mr. Dew's hand was on the cable 7" from the detector.

3. *Did Mr. Dew actually touch the TIP detector?*

Witnesses reported that in conversations with Mr. Dew immediately after the incident and during the next five days, Mr. Dew always stated that he did not touch the detector, even when specifically asked. Also, during every reenactment of the incident, he grabbed the cable, never touching the detector. The technician who was working with Mr. Dew during the incident stated that he did not see Mr. Dew touch the detector. He stated that he saw Mr. Dew re-insert the TIP and did not observe him touching the detector. However, this technician said that although he did not see Mr. Dew touch the detector, he could not absolutely state that he did not.

About five days later, Tuesday, July 10, 1990, Mr. Dew stated to one of the members of the original investigation team that he was now not sure that he did not touch the detector. At this time he told the investigator that he could have touched the detector, but if he did, he just brushed it before grabbing the cable. He demonstrated how this was possible and the investigator timed him. During this reenactment, the time that Mr. Dew's hand was in contact with the detector was about 0.4 seconds.

People familiar with this job and who had performed the job numerous times thought that it would not have been possible to grab the detector, release it, and then grab the cable. The cable is on a reel that is spring-loaded and would have been pulling on the cable. They all indicated that if you released the detector it would have retracted to the point of completely winding up on the take-up reel. This is further evidence that Mr. Dew did not touch the detector. The investigation team feels very confident that based on the evidence, Mr. Dew did not touch the detector and that was the assumption used in calculating the most probable dose to his hand. However, in calculating the upper bound of the dose, it was assumed that his hand was in contact with the detector for 0.5 seconds.

4. *How long was Mr. Dew's hand in contact with the cable/detector?*

Immediately following the incident, Mr. Dew repeatedly stated to management and HP personnel and demonstrated that his hand was in contact with the cable three seconds. Several times he demonstrated how he grabbed the cable and re-inserted it in the time required to count "1, 2, 3." During timed reenactments of the incident Mr. Dew always took three seconds or less to re-insert the TIP. However, later Mr. Dew indicated to one of the investigators that he, on his own, had attempted reenactment and he thought that it might have taken longer than three seconds, maybe about four seconds. Based on this last statement and to be conservative, the investigation team recommends using four seconds for the most probable time and three seconds for the lower bound. For the upper bound the four seconds in contact with the cable should be used; but as previously stated, it is also assumed that his hand was in contact with the detector for 0.5 seconds.

B. H. Webster
11/30/90

Attachment 11

Independent Evaluation of Dose Calculations

THE
ALEXANDER
CORPORATION

R.E. ALEXANDER
President

November 19,1990

Stephen A. Browne
Principal Specialist - Health Physics
Carolina Power and Light Company
P.O. Box 1551
Raleigh, NC 27602

Dear Mr. Browne:

At the request of Billy Webster, CP&L, I have reviewed your calculations of the dose received by the left hand of a CP&L employee on July 5, 1990. Details regarding this incident and the calculations appear in the document "Brunswick TIP Incident Dose Calculations" that you recently sent to me.

Regarding the gamma dose, which is only a small percentage of the total, I obtained and examined the Grove Engineering computer program MicroShield that was used for this calculation. The program is technically sound and is widely used in the nuclear power industry. The manner in which the program was used is correct. The best-estimate gamma dose at a tissue depth of 0.007 cm (about 1.4 rem) may be considerably overestimated since no correction for lack of electronic equilibrium at this depth was included in MicroShield. I discussed this problem with Dr. Daniel Reece, Texas A&M University. He is sending information to me regarding work on corrections of this type that has been completed at Battelle Northwest Laboratories. It may be feasible to make the correction if you so desire.

During my visit with you at Brunswick we carefully reviewed your calculation of the beta dose, which resulted in a best estimate of about 9.2 rems. Your use of equation 24 from Radiation Dosimetry, Hine and Brownell, appeared to me to be technically sound. The only reservation I had was about the manner in which the correction for self absorption by the source (cable in this case) is made by this equation. In a subsequent meeting that I attended with you, Mr. John Potter of the NRC requested a verification of your result; and at the request of CP&L I have conducted a rather thorough study.

13131 Maltese Lane • Fairfax, Virginia 22033
Telephone (703) 631-8878 Telefax (703) 631-8642

My first contact was with Sydney Porter who has developed a computer program for performing beta dose calculations. This program is based on tables published by W. G. Cross, Chalk River Laboratories ("Tables of Beta Ray Dose Distribution in Water, Air and Other Media", AECL-7617, 1982). Unfortunately, the capability of Porter's program is limited to infinitely thin plane source terms for which the question of beta absorption by the source itself does not arise. However, you had indicated to me that the correction provided by the Hine and Brownell equation was 0.5; thus the results of Porter's equation, multiplied by 0.5, would provide an estimate that could be compared with yours.

Using the Mn-56 total cable activity **q** of 5.241 Ci that you provided, the exterior cable circumference **C** of 0.785 inches, a length **L** of 9 feet, and a thickness **t** of 0.125 inches for the cable, and an infinite thickness τ of 2 mm for 2.85-MeV betas in iron, I estimated an infinitely thin source term of 6000 μCi/cm² as the necessary input for Porter's program. The following equation was used:

$$\sigma = \frac{q}{LC} \times \frac{\tau}{t}$$

The ratio **τ/t** eliminates Mn-56 that does not contribute to the surface dose rate. An activity distribution error was of necessity introduced in the conversion of the actual hollow cylinder to a rectangular plane. However, I believe the dose to the maximally exposed square centimeter of skin would be approximately the same from either geometry.

Using the previously mentioned input the following results, multiplied by 0.5 as in the case of the Hine and Brownell equation, were obtained:

Depth (mg/cm²)	Dose Rate (rads/sec)
7	6.7
20	5.0
99	2.3
112	2.2

Regarding the depths, a density of 1 g/cm³ was used for the rubber gloves worn by the exposed person (92 mg/cm²) and for tissue (7 mg/cm²). For an exposure of 4 seconds at 99 mg/cm², as used for your calculation, the estimate would be 9.2 rads. This result is the same as obtained from the Hine and Brownell equation. It adds confidence in your result but does not investigate the accuracy of the Hine and Brownell self-absorption correction.

To investigate the self-absorption phenomenon I contacted Dr. F. H. Attix, who recommended a Monte Carlo simulation using a code written at the University of Wisconsin under the supervision of Dr. Thomas R. Mackie. Dr. Mackie agreed to perform the calculation, using input data that I provided in a letter approved by you and dated October 24, 1990, Attachment 1. His results were sent to me on November 12, 1990, Attachment 2. At 100 mg/cm^2 the dose rate is shown to be 131.5 rads/sec per Ci of Mn-56 per gram of iron, with a standard deviation of 9.3 rads/sec. The dose rate associated with a specific activity of 0.0189 Ci/gm is 2.485 rads/sec. For a 4-second exposure the dose would be approximately 9.9 rads.

The Hine and Brownell equation was developed before current Monte Carlo methods were computerized and does not account for self absorption with the accuracy of the Monte Carlo simulation. For this reason I recommend acceptance, for purposes of compliance demonstration, of the 9.9-rad beta dose estimate at a tissue depth of 7 mg/cm^2, the depth required by 10 CFR Part 20. For purposes of the CP&L medical record, I recommend recording also the dose at a tissue depth of 40 mg/cm^2, the depth at which the cells at risk (the basal cell layer) are likely to be located (ICRP Report 23). At a total depth of 130 mg/cm^2, Dr. Mackie reports a dose rate of 110.1 rads/sec per Ci/gm, which would be 2.08 rads/sec from the cable. Thus the recorded beta dose would be 8.3 rads. If the actual depth to the basal cell layer is desired, it may be possible to obtain it through examination by a dermatologist. Recomputation of the dose might then be in order.

Please note that my analysis did not include review of assumptions such as the neutron irradiation time for the cable in the reactor core, the activation determination, or details of the exposure such the location of the hand on the source and the time of exposure.

Please call on me if I can be of further assistance.

Sincerely,

R E Alexander

Robert E. Alexander

Enclosures:
Attachment 1, letter to Mackie
Attachment 2, response from Mackie

cc: J. Michael McGarry
Winston and Strawn

THE ALEXANDER CORPORATION

R.E. ALEXANDER
President

October 24, 1990 10/24/90

Dr. Thomas R. Mackie
Department of Medical Physics
University of Wisconsin
1300 University Avenue
Room 1530
Madison, Wisconsin 53706

Bob,
This looks good — Please proceed. I am also sending you 2 pages from ICRP 23.
Steve Browne

Dear Dr. Mackie:

In connection with our recent discussion about a beta radiation skin dose calculation that you expressed willingness to perform, I am pleased to say that my client has authorized the work. To expedite the administrative aspects, the work will be performed for my corporation; and your invoice should be directed to me at the address shown on the letterhead.

The information that you will need is provided below:

1. The radionuclide is Mn-56.
2. The quantity to be used is 1 Ci.
3. The radionuclide is an activated impurity uniformly distributed in an Fe slab of infinite area and of thickness greater than the range of the maximum Mn-56 beta (2.85 MeV).
4. The beta dose rate is to be calculated in units of rad/sec.
5. Exposure configuration: the palm of the hand is pressed against a flat Fe slab.
6. The beta dose rate is to be provided at the absorber depths listed below, assuming for each depth an absorber density of 1 g/cm^3:

0	mg/cm^2
7	"
99	"
114	"
129	"

I will be expected to provide a report to my client in sufficient detail to satisfy any regulatory and legal needs that may arise. For this reason I would appreciate receiving from you a brief description of the computer program you will use. The target audience for this description would be health physics

13131 Maltese Lane • Fairfax, Virginia 22033
Telephone (703) 631-8878 Telefax (703) 631-8642

personnel employed by the Nuclear Regulatory Commission (NRC). A copy of your CV would also be beneficial for this file.

In accordance with our telephone conversation, I have informed my client (1) that the calculations will be performed by you or under your direct supervision and that the results will be authenticated by your signature, (2) that the fee will be based on a rate of $100 per hour, or $500 per day if the time requirement is more extensive, and (3) that 1 day might be a good estimate for the calculation as I described it over the telephone.

I am very happy to have this opportunity to work with you. My friend Frank Attix has spoken very highly of your capability and standing in the beta dosimetry field; it is very fortunate that you are in the position to help us at this time. The NRC has requested a dose report from my client within 2 weeks, and it is my understanding from you that this schedule is compatible with the amount of time you are likely to need.

Please call me if additional details regarding the exposure are needed for your calculations.

Sincerely,

Robert E. Alexander

UNIVERSITY OF
WISCONSIN-MADISON
MEDICAL SCHOOL

Nov. 12, 1990

Robert E. Alexander
The Alexander Corporation
13131 Maltese Lane
Fairfax, Virginia 22033

Dear Dr. Alexander,

Find enclosed the results of a Monte Carlo simulation involving an exposure from β^- particles emitted from ^{56}Mn. I apologize for the delay of the weekend, but we wanted to do some additional tests of the simulation to verify that the simulation was free of any systematic errors.

The Monte Carlo code used was EGS4 (Electron Gamma Shower Version 4) originally written by Ralph Nelson and colleagues at the Stanford Linear Accelerator Center and modified and benchmarked for low energy transport by David Rogers and colleagues at the National Research Council of Canada. The specific user code is called XYZDOS was written by David Rogers and Alex Bielajew and modified, under my supervision, by Mark Holmes to model radioactive sources. Collaboration was also provided by two other students: Tim Holmes and Douglas Simpkin. As agreed during our telephone conversation additional documentation describing this code can be supplied by us, however, EGS4 is widely described in the literature (eg. Nucl. Inst. and Methods, Medical Physics, Phys. Med. Biol.)

In addition to the specific details of the simulation we conducted several tests of the code to ensure its correctness. Specifically we:

- tested that energy was being conserved for different numbers of histories (simulated particles)
- tested that for conditions of charged particle equilibrium that the simulated dose rate in homogeneous water and Fe phantoms agreed with the equation:

$$\left(\frac{dD}{dt}\right)_\beta = \frac{A}{M}\Sigma_i(\Delta_{\beta^-})_i$$

where $(\frac{dD}{dt})_\beta$ is the dose rate, $\frac{A}{M}$ is the activity per unit mass and $(\Delta_{\beta^-})_i$ is the equilibrium dose rate constants for bins describing the beta spectrum for ^{56} Mn, the sum of which is the mean energy of beta particles per decay (0.832 MeV or 4.91 $\times 10^2$ g · rad/(Ci · s).

- ensured that the β^- were being emitted uniformly in the source region and isotropically distributed in direction.

According to your specifications of the problem outlined in your FAX of October 24 and in our telephone conversations we simulated the geometry described by the accompanying diagram. Briefly, it consists of a 12 cm × 12 cm slab of iron (density = 7.86 g/cm^3) that contains a uniform isotropically emitting source of ^{56}Mn. The thickness of the slab is 0.5 cm which is greater than the range of the betas in iron. The scoring region consisted of 20 slabs 8 cm × 8 cm by 0.01 cm thick centered beneath the Fe slab. The scoring region was surrounded by 2 cm of water to the sides and 1.8 cm of water below to ensure scatter equilibrium to the scoring region. Only the dose from beta particles was simulated (the dose from gamma or internal bremsstrahlung is not to be included).

The tabulation of Browne and Firestone (enclosed) was felt to be too coarse so the beta spectrum of ^{56}Mn was obtained from Douglas Simpkin using a code described in the literature (Simpkin and Mackie, Med. Phys., 1990). It consisted of 49 spectral bins and a plot of the spectrum is enclosed including a comparison with Browne and Firestone. The simulation consisted of running 1000 simulated decays for each of the 49 bins for a total of 49,000 histories. The probability of emission from each of the bins (as expressed in numbers of histories per 10,000 decays) was used to weight histories starting from each of the bins. The simulation was run on a Sun Sparcstion-1 computer.

The dose rate per Ci/g $\frac{dD/dt}{(A/M)}$ for any of the scoring region slabs was obtained from the following equation:

$$\frac{dD/dt}{(A/M)}[rad \cdot g/(Ci \cdot s)] = 3.7 \times 10^{10} Bq/Ci \cdot \frac{100rad}{Gy} \cdot M_{source}[g] \cdot \frac{D_{score}[Gy]}{N_{decay}}$$

where $D_{score}[Gy]$ is the dose in Grays scored in a water slab, $M_{source}[g]$ is the mass of the source region in grams which was 565.9 g, and N_{decay} is the number of simulated decays in the source region.

For the particular geometry used the following equation is more convenient:

$$\frac{dD/dt}{(A/M)}[rad \cdot g/(Ci \cdot s)] = 2.09 \times 10^{15}[\frac{rad \cdot g/(Ci \cdot s)}{Gy/decay}] \cdot \frac{D_{score}}{N_{decay}}[Gy/decay]$$

The tabulated and graphed results are enclosed. The dose rate in rad/s per Ci/g from beta particle emission in the first scoring region past the interface (the interface is located at 0.5 cm) is 2.49×10^2 g · rad / (Ci · s) and rapidly falls to values between about 1.2 to 0.6×10^2 g · rad / (Ci · s) at 0.1 cm to 0.2 cm past the interface, respectively. The percent statistical uncertainty (100 × standard deviation/value) is typically less than 5%.

The value near the boundary is within 2 % of what one would expect from the simple dosimetric approximation of assuming an equilibrium spectrum of betas from a semi-infinite slab source (i.e. half the equilibrium dose rate or $\frac{4.91}{2} \times 10^2$ g · rad/(Ci · s). This is fortuitous for two reasons. The accuracy of the simulation is not within 2%. The simple analytic estimation is very crude. Including the ratio of mass collision stopping powers between water and iron would have increased the crude estimate by about 30 to 40% and including the lack of an equilibrium scatter would tend to decrease the result by a similar amount. Of course the Monte Carlo simulation takes both of these effects into account implicitly.

This report is being sent by FAX, but will be followed up with a letter that will include a longer run with less uncertainty. At that time, I will also include the raw output from the Monte Carlo simulation which lists some of the details of the particle transport and a reprint of the Simpkin and Mackie paper. I hope that you find these results useful and please let me know if you have any other questions or concerns.

Accompanying the letter will be an invoice from the UW Medical Physics Department for $2,000. It will fund for travel expenses for graduate students working in our radiation dosimetry research group.

Best regards. Yours sincerely,

T R Mackie

T.R. Mackie
Assistant Professor
(608) 262-7358

cc: Mark Holmes, Tim Holmes, Douglas Simpkin

Table of Radioactive Isotopes

Edgardo Browne and Richard B. Firestone

Virginia S. Shirley, Editor

Lawrence Berkeley Laboratory
University of California

A Wiley-Interscience Publication
JOHN WILEY & SONS
New York · Chicheste · Brisbane · Toronto · Singapore

$^{56}_{25}$Mn(2.5785 6 h)

Mode: β-
Δ: -56908.4 15 keV
SpA: 2.1702×10^{7} Ci/g
Prod: ^{55}Mn(n,γ)

Photons (^{56}Mn)

⟨γ⟩=1692 23 keV

γmode	γ(keV)	γ(%)†
γ[M1+E2]	787.80 4	0.00034 4
γ E2	846.812 20	98.9 3
γ[M1+E2]	1037.879 19	0.040 3
γ E2	1238.317 21	0.099 10
γ[M1+E2]	1360.29 3	0.0048 3
γ M1+3.5%E2	1810.80 4	27.2 7
γ M1+4.0%E2	2113.19 8	14.3 4
γ[E2]	2276.[illegible] 3	0.00034 7
γ[M1+E2]	2522.95 9	0.99 3
γ[M1+E2]	2598.57 3	0.0188 20
γ[E2]	2657.58 4	0.653 20
γ[E2]	2959.96 6	0.306 10
γ[E2]	3369.72 9	0.170 9

† <0.1% uncert(syst)

Continuous Radiation (^{56}Mn)

⟨β-⟩=830 keV;⟨IB⟩=1.9 keV

E_{bin}(keV)		⟨ ⟩(keV)	(%)
0 - 10	β-	0.0344	0.69
	IB	0.031	
10 - 20	β-	0.104	0.70
	IB	0.030	0.21
20 - 40	β-	0.431	1.43
	IB	0.059	0.20
40 - 100	β-	3.29	4.66
	IB	0.164	0.25
100 - 300	β-	35.0	17.4
	IB	0.44	0.25
300 - 600	β-	101	23.0
	IB	0.45	0.106
600 - 1300	β-	247	27.0
	IB	0.54	0.063
1300 - 2500	β-	429	24.5
	IB	0.17	0.0108
2500 - 2849	β-	14.3	0.55
	IB	0.00036	1.42 $\times 10^{-5}$

$^{56}_{26}$F[illegible] [illegible]ble)

Δ: [illegible].1 15 keV
%: 91.72 30

$^{56}_{27}$Co(77.7 5 d)

Mode: ε
Δ: -56038.0 25 keV
SpA: 3.001×10^{4} Ci/g
Prod: ^{56}Fe(p,n); ^{55}Mn(α,3n); daughter ^{56}Ni; ^{56}Fe(d,2n); ^{58}Ni(d,α)

Photons (^{56}Co)

⟨γ⟩=3378 32 keV

γmode	γ(keV)	γ(%)†
Fe L_{ℓ}	0.615	0.031 8
Fe L_{η}	0.628	0.021 3
Fe L_{α}	0.705	0.29 7
Fe L_{β}	0.726	0.22 6
Fe $K_{\alpha 2}$	6.391	7.3 4
Fe $K_{\alpha 1}$	6.404	14.4 7
Fe $K_{\beta 1}$'	7.058	2.58 13
γ[M1+E2]	263.46 5	0.021 4
γ[M1+E2]	411.23 5	0.025 5
γ[M1+E2]	486.86 10	0.050 10
γ[M1+E2]	674.69 4	0.030 10
γ[M1+E2]	733.64 4	0.192 22
γ[M1+E2]	787.80 4	0.307 7
γ E2	846.812 20	99.9
γ[M1+E2]	896.63 8	0.075 10
γ[M1+E2]	977.48 4	1.40 3
γ[M1+E2]	997.10 4	0.14 3
γ[M1+E2]	1037.879 19	14.1 3
γ[M1+E2]	1089.11 8	0.050 20
γ[M1+E2]	1140.46 6	0.126 15
γ[E2]	1160.09 8	0.091 10
γ[M1+E2]	1175.15 3	2.26 6
γ[M1+E2]	1199.03 5	0.043 11
γ E2	1238.317 21	67.0 13
γ[M1+E2]	1272.08 10	0.0200 10
γ	1335.59 6	0.1209 24
γ[M1+E2]	1360.29 3	4.29 9
γ[M1+E2]	1442.86 5	0.174 4
γ[E2]	1462.48 5	0.072 6
γ[E2]	1640.53 4	0.063 3
γ[M1+E2]	1771.51 4	15.5 3
γ M1+3.5%E2	1810.80 4	0.650 20
γ[M1+E2]	1963.98 7	0.702 14
γ[M1+E2]	2015.34 4	3.03 6
γ[M1+E2]	2034.96 4	7.77 16
γ M1+4.0%E2	2113.19 8	0.376 8
γ[M1+E2]	2213.00 5	0.376 8
γ[E2]	2275.17 3	0.120 18
γ	2373.44 6	0.061 8
γ[M1+E2]	2522.95 9	0.054 6
γ[M1+E2]	2598.57 3	16.7 3
γ[E2]	2657.58 4	0.0156 7
γ[E2]	2959.96 6	0.0080 3
γ[M1+E2]	3009.78 4	1.03 9
γ[M1+E2]	3202.25 6	3.02 21
γ[M1+E2]	3253.60 4	7.4 3
γ[E2]	3273.23 4	1.73 12
γ[E2]	3369.72 9	0.0094 5
γ[E2]	3451.27 4	0.89 9
γ[M1+E2]	3548.2 1	0.173 17
γ	3600.86 21	0.0150 20
γ	3611.70 7	0.0078 10

† <0.1% uncert(syst)

Atomic Electrons (^{56}Co)

⟨e⟩=3.6 3 keV

e_{bin}(keV)	⟨e⟩(keV)	e(%)
1	0.47	65 7
5	0.170	3.1 3
6	2.5	43 4
256 - 263	0.00041	~0.00016
404 - 411	0.00018	4.5 19 $\times 10^{-5}$
480 - 486	0.00026	5.5 20 $\times 10^{-5}$
668 - 674	9.0 $\times 10^{-5}$	1.3 3 $\times 10^{-5}$
727 - 733	0.00051	7.0 13 $\times 10^{-5}$
781 - 787	0.00073	9.3 16 $\times 10^{-5}$
840	0.225	0.0268 8
846 - 890	0.0219	0.00259 7
970 - 996	0.0027	0.00028 1
1031 - 1037	0.0234	0.00227 23
1082 - 1088	7.8 $\times 10^{-5}$	7 3 $\times 10^{-6}$
1133 - 1174	0.0036	0.00031 3
1192 - 1198	6.1 $\times 10^{-5}$	5.1 11 $\times 10^{-6}$
1231	0.0891	0.00724 20

Atomic Electrons (^{56}Co)

(continued)

e_{bin}(keV)	⟨e⟩(keV)	e(%)
1237 - 1271	0.00855	0.000691 19
1328 - 1360	0.0054	0.00040 3
1436 - 1462	0.000290	2.01 12 $\times 10^{-5}$
1633 - 1640	6.8 $\times 10^{-5}$	4.15 24 $\times 10^{-6}$
1764 - 1810	0.0156	0.00089 8
1957 - 2034	0.0100	0.000496 23
2106 - 2112	0.000309	1.47 4 $\times 10^{-5}$
2206 - 2275	0.000405	1.82 10 $\times 10^{-5}$
2366 - 2373	3.9 $\times 10^{-5}$	1.7 4 $\times 10^{-6}$
2516 - 2598	0.0123	0.00047 3
2650 - 2657	1.15 $\times 10^{-5}$	4.34 25 $\times 10^{-7}$
2953 - 3009	0.00069	2.31 22 $\times 10^{-5}$
3195 - 3273	0.0078	0.000241 13
3363 - 3451	0.00057	1.65 16 $\times 10^{-5}$
3541 - 3611	0.000117	3.3 3 $\times 10^{-6}$

Continuous Radiation (^{56}Co)

⟨β+⟩=120 keV;⟨IB⟩=0.44 keV

E_{bin}(keV)		⟨ ⟩(keV)	(%)
0 - 10	β+	7.9 $\times 10^{-5}$	0.00100
	IB	0.00[illegible]6	
10 - 20	β+	0.00[illegible]30	0.0081
	IB	0.00[illegible]1	0.036
20 - 40	β+	0.01[illegible]3	0.051
	IB	0.00[illegible]9	0.034
40 - 100	β+	0.331	[illegible]44
	IB	0.028	0.[illegible]43
100 - 300	β+	6.8	3.[illegible]4
	IB	0.086	0.0[illegible]7
300 - 600	β+	28.6	6.3
	IB	0.120	0.028
600 - 1300	β+	83	9.7
	IB	0.143	0.017
1300 - 2481	β+	1.70	0.127
	IB	0.046	0.0028
	Σβ+		20

$^{56}_{28}$Ni(6.10 2 d)

Mode: ε
Δ: -53902 11 keV
SpA: 3.822×10^{5} Ci/g
Prod: ^{54}Fe(α,2n); ^{56}Fe(^{3}He,3n)

Photons (^{56}Ni)

⟨γ⟩=1721 20 keV

γmode	γ(keV)	γ(%)†
Co L_{ℓ}	0.678	0.042 11
Co L_{η}	0.693	0.027 7
Co L_{α}	0.776	0.44 11
Co L_{β}	0.799	0.34 9
Co $K_{\alpha 2}$	6.915	10.1 5
Co $K_{\alpha 1}$	6.930	19.8 10
Co $K_{\beta 1}$'	7.649	3.60 18
γ M1+0.03%E2	158.39 3	98.8
γ M1	269.512 17	36.5 8
γ E2	480.452 17	36.5 8
γ M1	749.962 19	49.5 12
γ M1(+0.08%E2)	811.86 3	86.0 17
γ E2	1561.81 3	14.0 6

† 2.0% uncert(syst)

****

intout of file: mn56spec.dat , with present directory =
\GRAPH\DATA
Date of printout: 10-31-1990 @ 11:49:57

****

for 10^4 decays

0.0284860	405
0.0854580	454
0.1424300	486
0.1994020	502
0.2563740	504
0.3133460	497
0.3703180	482
0.4272900	456
0.4842620	423
0.5412340	384
0.5982060	343
0.6551780	305
0.7121500	273
0.7691220	249
0.8260940	228
0.8830660	208
0.9400380	193
0.9970100	185
1.0539820	184
1.1109539	186
1.1679260	186
1.2248980	186
1.2818700	185
1.3388419	183
1.3958139	180
1.4527860	176
1.5097580	172
1.5667299	166
1.6237019	160
1.6806740	154
1.7376460	146
1.7946179	138
1.8515899	130
1.9085619	121
1.9655340	112
2.0225058	102
2.0794780	93
2.1364498	83
2.1934218	73
2.2503939	64
2.3073659	54
2.3643379	45
2.4213099	37
2.4782820	29
2.5352540	21
2.5922258	15
2.6491978	9
2.7061698	5
2.7631419	2
2.8201139	0

Calc'd ave β energy = .832 MeV
(vs .830 MeV from Kocher)

Δ = 1.768 g rad/μCi-hr
(vs 1.77 g rad/μCi-hr from Kocher)

This data used for the beta spectrum

↑ energy of bin (MeV)

↑ # β^- started for 10^4 decays.

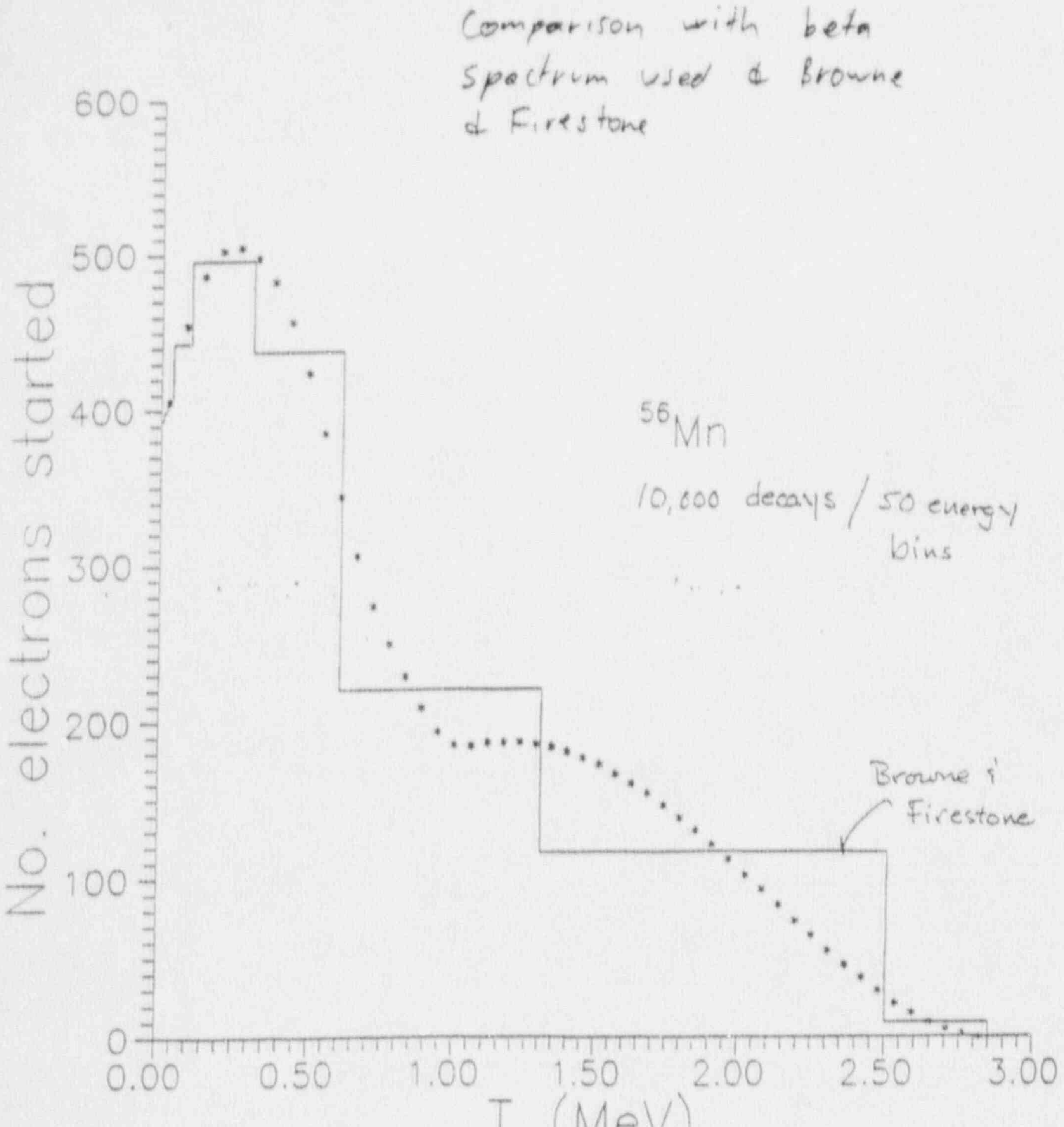
Comparison with beta spectrum used & Browne & Firestone
600
500
400
300
200
100
0
No. electrons started
0.00
0.50
1.00
1.50
2.00
2.50
3.00
T (MeV)
^{56}Mn
10,000 decays / 50 energy bins
Browne & Firestone

Distribution of Dose About a Point ^{56}Mn Source in water with Inverse-Square Removed and the X-axis scaled to units of X_{90}

(Used for a test only)

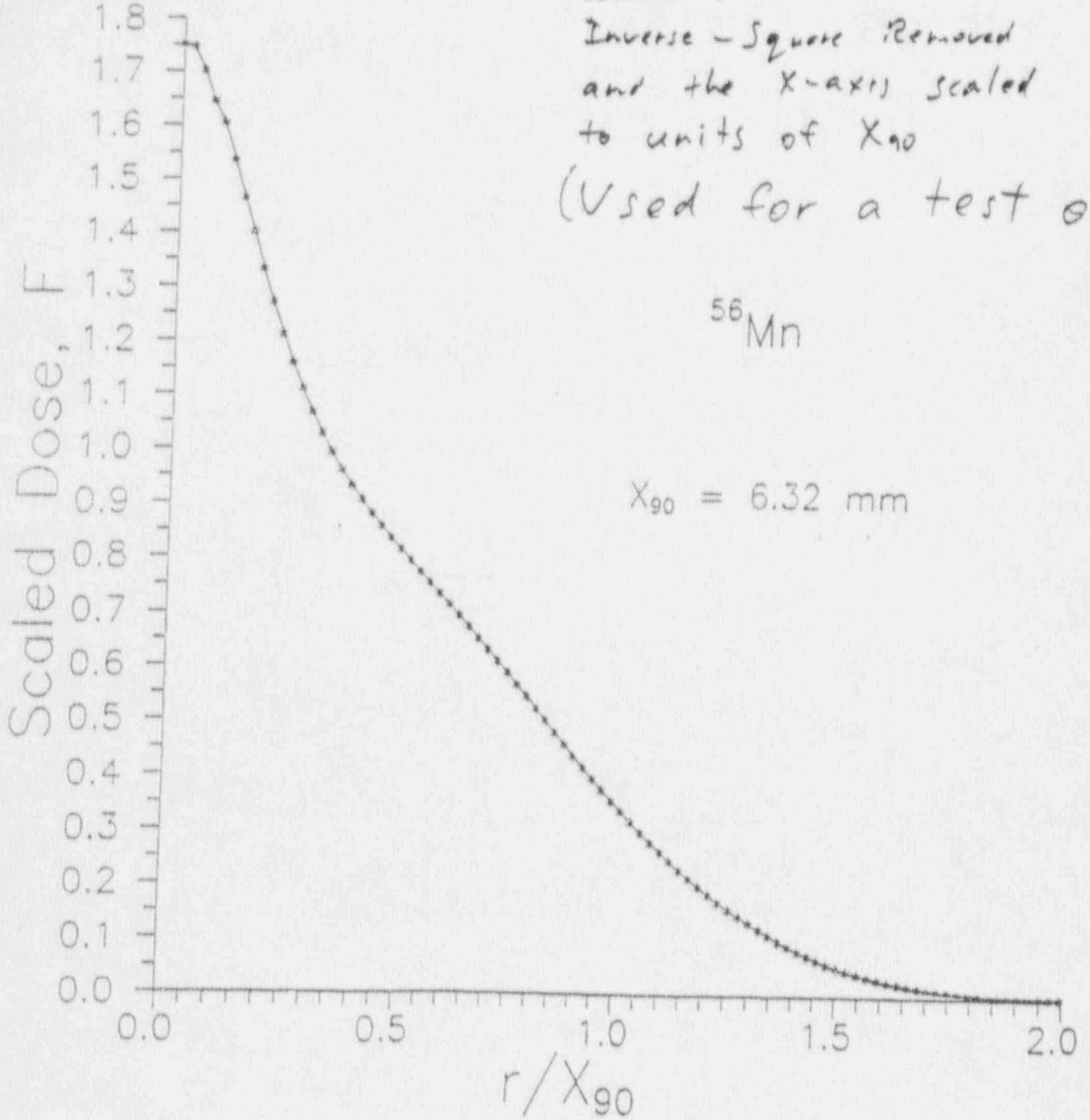

The Phantom Geometry

Note: All Dimensions
in centimeters.

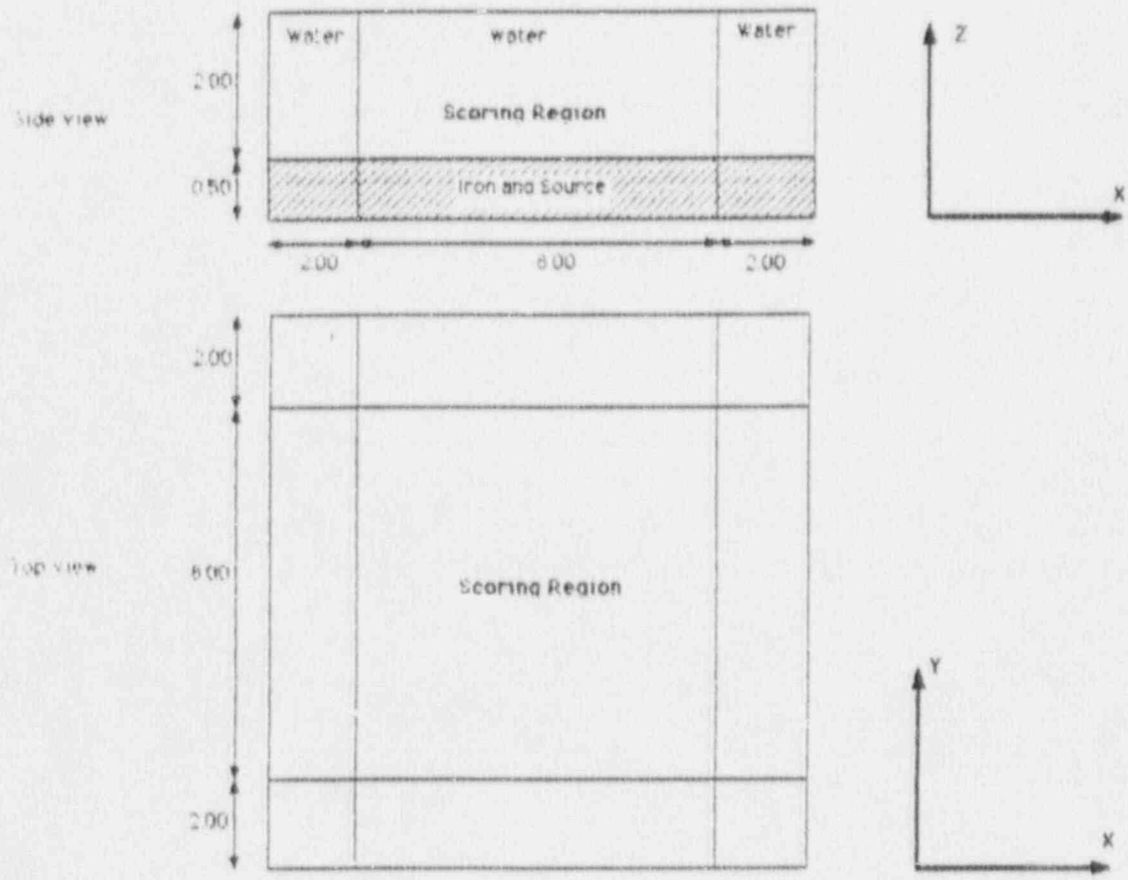

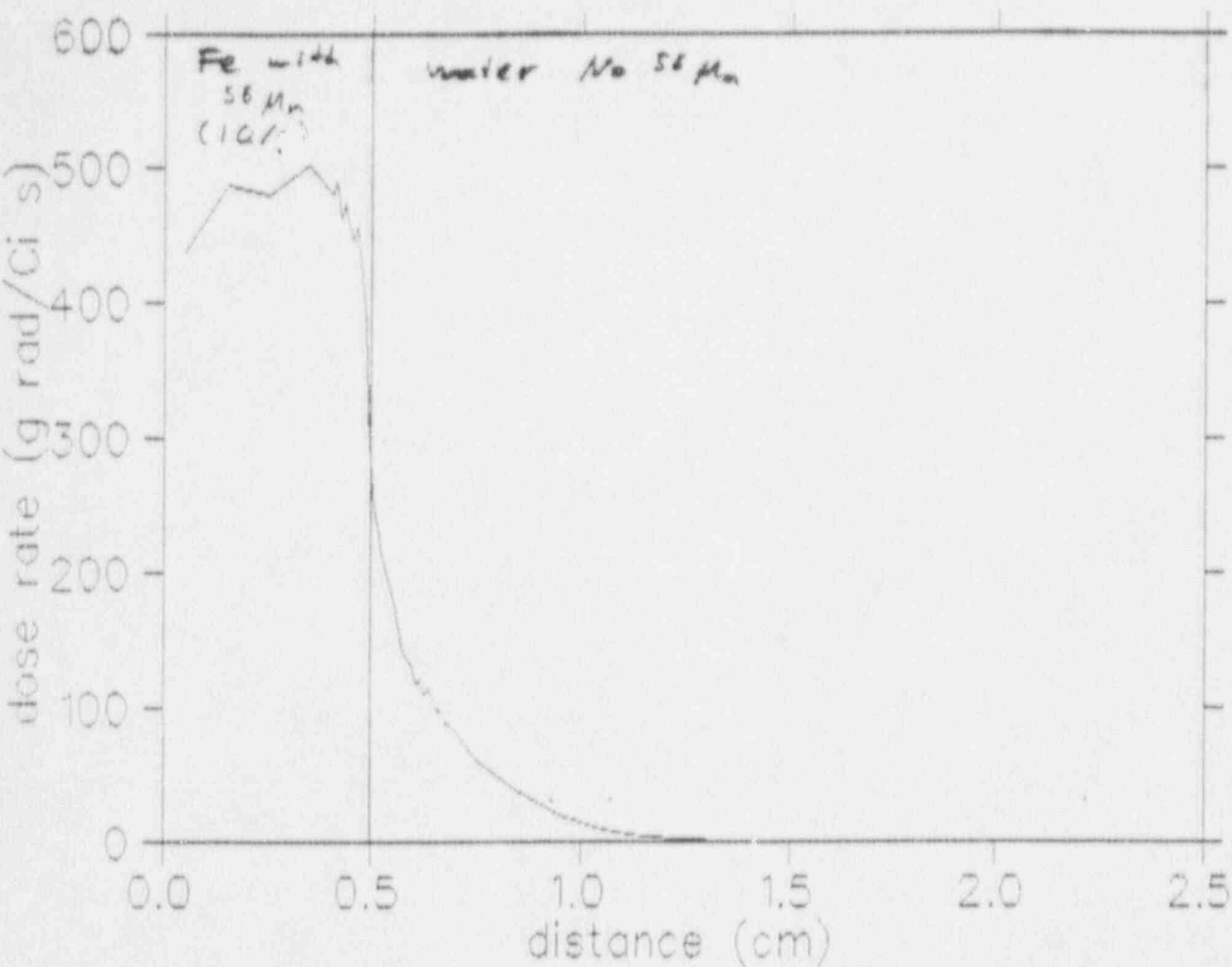

1,000 decays/bin

1,000 decays / bin

Region Bound (cm)	Dose/Dis (Gy/Dis)	Dose/Dis St. Dev (%)	Bin Center	Dose Rate (g rad / Ci s)	Dose Rate St. Dev (g rad / Ci s)	
0.1	2.089	1.4	0.05	437.4	61.2	
0.2	2.329	2.2	0.15	487.6	10.7	
0.3	2.292	1.8	0.25	479.9	8.6	
0.4	2.397	1.7	0.35	501.9	8.5	
0.41	2.292	3.2	0.405	479.9	15.3	
0.42	2.336	3.9	0.415	489.1	19.0	
0.43	2.207	2.4	0.425	462.1	11.0	
0.44	2.262	4.6	0.435	473.6	21.7	
0.45	2.181	3.5	0.445	456.7	15.9	
0.46	2.13	3.5	0.455	446.0	15.6	
0.47	2.179	4.4	0.465	456.2	20.0	
0.48	2.005	3.6	0.475	419.8	15.1	
0.49	1.842	3.5	0.485	385.7	13.5	Fe
0.5	1.417	3.5	0.495	296.7	10.3	
---	---	---	---	---	---	
0.51	1.19	6.3	0.505	249.1	15.6	Water
0.52	1.119	7.1	0.515	234.3	16.6	
0.53	1.017	5.6	0.525	212.9	11.9	
0.54	0.9545	6.4	0.535	199.8	12.7	
0.55	0.8945	5.6	0.545	187.3	10.4	
0.56	0.8297	7.7	0.555	173.7	13.3	
0.57	0.7429	4.2	0.565	155.5	6.5	
0.58	0.6767	7.4	0.575	141.7	10.4	
0.59	0.6458	6.9	0.585	135.2	9.3	
0.6	0.6284	7.1	0.595	131.5	9.3	
0.61	0.5662	8.9	0.605	118.5	10.5	
0.62	0.575	7.2	0.615	120.4	8.6	
0.63	0.5258	8.3	0.625	110.1	9.1	
0.64	0.547	7.3	0.635	114.5	8.3	
0.65	0.4939	7.6	0.645	103.4	7.8	
0.66	0.4703	8.2	0.655	98.4	8.0	
0.67	0.4712	7.7	0.665	98.6	7.5	
0.68	0.4263	8.7	0.675	89.2	7.7	
0.69	0.4217	7.3	0.685	88.3	6.4	
0.7	0.4114	6.9	0.695	86.1	5.9	
0.8	0.2998	5.8	0.75	62.7	3.6	
0.9	0.1833	9.7	0.85	38.3	3.7	
1	0.09706	15.3	0.95	20.3	3.1	
1.1	0.0482	12.0	1.05	10.0	1.2	
1.2	0.0173	22.7	1.15	3.6	.8	
1.3	0.007569	26	1.25	1.5	.4	
1.4	0.0043[illegible]	30.5	1.35	.9	.2	
1.5	0.00141	40.1	1.45	.3	.1	
1.6	0.000685	64.2	1.55	.1	.0	
1.7	0.000437	81.8	1.65	.1	.0	
1.8	0.000802	58.8	1.75	.1	.0	
1.9	0.001768	57.1	1.85	.4	.2	
2	0.000753	73.6	1.95	.1	.1	
2.1	0.003085	56	2.05	.6	.3	
2.2	0.002475	61.2	2.15	.5	.3	
2.3	0.001004	96.4	2.25	.2	.2	
2.4	0.001452	85	2.35	.3	.2	
2.5	0.000146	99.9	2.45	.0	.0	

J K Moore

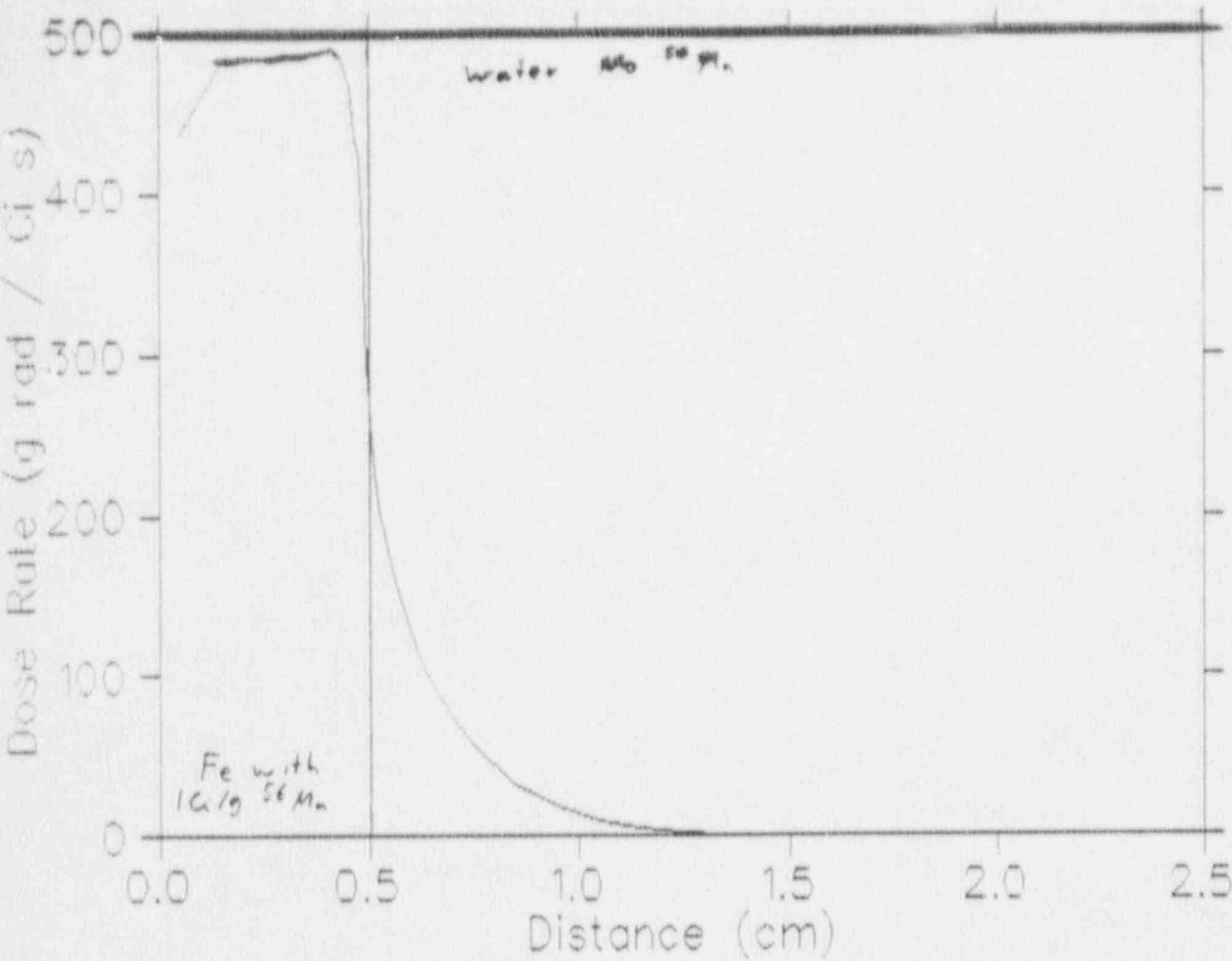

10,000 decays / bin × 49 bins = 490,000 histories

10,000 decays / bin

Upper Bound (cm)	Dose/Dis (Gy/Dis) (*10^-13)	Dose/Dis St. Dev. (%)	Center (cm)	Dose Rate (g rad / Ci s)	Dose Rate St. Dev. (g rad / Ci s)	
0.10	2.090	0.3	0.050	437.6	1.3	
0.20	2.307	0.5	0.150	483.1	2.4	
0.30	2.319	0.4	0.250	485.6	1.9	
0.40	2.326	0.2	0.350	487.1	9.7	
0.41	2.339	1.2	0.405	489.8	5.9	
0.42	2.344	1.2	0.415	490.9	5.9	
0.43	2.331	1.1	0.425	488.1	5.4	
0.44	2.325	1.5	0.435	486.9	7.3	
0.45	2.274	1.8	0.445	476.2	8.6	
0.46	2.230	1.4	0.455	467.0	6.5	
0.47	2.095	0.8	0.465	438.7	3.5	
0.48	2.014	0.5	0.475	421.7	2.1	
0.49	1.794	1.4	0.485	375.7	5.3	
0.50	1.395	1.6	0.495	292.1	4.7	Fe
0.51	1.182	1.8	0.505	247.5	4.5	Water
0.52	1.049	1.6	0.515	219.7	3.5	
0.53	0.9684	1.2	0.525	202.8	2.4	
0.54	0.9039	1.5	0.535	189.3	2.8	
0.55	0.8483	2.0	0.545	177.6	3.6	
0.56	0.7894	1.3	0.555	165.3	2.1	
0.57	0.7425	1.9	0.565	155.5	3.0	
0.58	0.7072	2.6	0.575	148.1	3.9	
0.59	0.6642	2.7	0.585	139.1	3.8	
0.60	0.6279	2.3	0.595	131.5	3.0	
0.61	0.5963	2.5	0.605	124.9	3.1	
0.62	0.5448	2.8	0.615	114.1	3.2	
0.63	0.5257	1.9	0.625	110.1	2.1	
0.64	0.4889	2.2	0.635	102.4	2.3	
0.65	0.4702	3.5	0.645	98.5	3.4	
0.66	0.4542	3.8	0.655	95.1	3.6	
0.67	0.4236	2.4	0.665	88.7	2.1	
0.68	0.4062	2.9	0.675	85.1	2.5	
0.69	0.3825	4.2	0.685	80.1	3.4	
0.70	0.3636	4.4	0.695	76.1	3.4	
0.80	0.2741	3.1	0.750	57.4	1.8	
0.90	0.1564	3.4	0.850	32.8	1.1	
1.00	0.08974	3.4	0.950	18.79	0.64	
1.10	0.04546	6.0	1.050	9.52	0.57	
1.20	0.02002	6.3	1.150	4.19	0.26	
1.30	0.01070	12.0	1.250	2.24	0.27	
1.40	0.005174	15.2	1.350	1.08	0.17	
1.50	0.003473	22.5	1.450	0.73	0.16	
1.60	0.002705	35.4	1.550	0.57	0.20	
1.70	0.001906	17.2	1.650	0.399	0.069	
1.80	0.002143	33.1	1.750	0.45	0.15	
1.90	0.001395	37.7	1.850	0.29	0.11	
2.00	0.001403	41.9	1.950	0.29	0.12	
2.10	0.000654	45.8	2.050	0.137	0.063	
2.20	0.001718	14.6	2.150	0.360	0.053	
2.30	0.001507	22.3	2.250	0.316	0.070	
2.40	0.001719	32.7	2.350	0.36	0.12	
2.50	0.000666	39.6	2.450	0.139	0.055	

Output from the first run

```
1                        NRCC USER CODE ICDOS(V1.0) USING EGS4 AND PRESTA

 GEOMETRY IS A RECTILINEAR VOLUME, ORIGIN IN BOTTOM LEFT,X-Y PLANE ON
                       THE PAGE AND Z AXIS INTO THE PAGE

 ------------------------------------------------------------------------------
 TITLE: +   The dose to big cube of water perfused with a Mg-56 source spectrum
 ------------------------------------------------------------------------------
 NUMBER OF MEDIA: +                      2
 MEDIUM  1:  +                           FE
 MEDIUM  2:  +                           H2O521
 ECUT,PCUT,ESTPE(1 to 2):  +                      0.515      0.515      0.020      0.020

 # REGIONS IN X,Y,Z DIRECTIONS  (IF<0,IMPLIES # GROUPS OF REG): +      3      3

                       INPUT BOUNDARIES IN THE X DIRECTION
 SMALL BOUNDARY FOR REGION(  1)   +                0.000
 SMALL BOUNDARY FOR REGION(  2)   +                2.000
 SMALL BOUNDARY FOR REGION(  3)   +               10.000
 OUTER BOUNDARY FOR REGION(  3)   +               12.000

                       INPUT BOUNDARIES IN THE Y DIRECTION
 SMALL BOUNDARY FOR REGION(  1)   +                0.000
 SMALL BOUNDARY FOR REGION(  2)   +                2.000
 SMALL BOUNDARY FOR REGION(  3)   +               10.000
 OUTER BOUNDARY FOR REGION(  3)   +               12.000

                       INPUT BOUNDARIES IN THE Z DIRECTION
 INITIAL BOUNDARY: +        0.000
 WIDTH IN THIS GROUP, NO. OF REGIONS IN GROUP: +        0.100     4
 WIDTH IN THIS GROUP, NO. OF REGIONS IN GROUP: +        0.010    30
 WIDTH IN THIS GROUP, NO. OF REGIONS IN GROUP: +        0.100    18
 BOUNDARIES
       0.000        0.100        0.200        0.300        0.400        0.410
       0.420        0.430        0.440        0.450        0.460        0.470
       0.480        0.490        0.500        0.510        0.520        0.530
       0.540        0.550        0.560        0.570        0.580        0.590
       0.600        0.610        0.620        0.630        0.640        0.650
       0.660        0.670        0.680        0.690        0.700        0.800
       0.900        1.000        1.100        1.200        1.300        1.400
       1.500        1.600        1.700        1.800        1.900        2.000
       2.100        2.200        2.300        2.400        2.500
0TOTAL # REGIONS INCLUDING EXTERIOR =  469
0INPUT GROUPS OF REGIONS FOR WHICH DENSITY AND MEDIUM ARE NOT DEFAULTS
 LOWER,UPPER I, J, K,  MEDIUM, DENSITY+(  1   3)(  1   3)(  1  14)   1      7.860
  Things have been forced to comply with the following geometry
  I=1..3,J=1..3,K=1..14  rho=7.86 med=1 (Fe)
  I=1..3,J=1..3,K=15..52 rho=1.00 med=2 (H2O)
 LOWER,UPPER I, J, K,  MEDIUM, DENSITY+(  1   3)(  1   3)(  1  52)   2      1.000
  Things have been forced to comply with the following geometry
  I=1..3,J=1..3,K=1..14  rho=7.86 med=1 (Fe)
  I=1..3,J=1..3,K=15..52 rho=1.00 med=2 (H2O)
 LOWER,UPPER I, J, K,  MEDIUM, DENSITY0INPUT GROUPS OF REGIONS FOR WHICH ECUT AN
 LOWER,UPPER I, J, K,  ECUT, PCUT0ENTER 3 PAIRS DEFINING LOWER,UPPER X,Y,Z INDIC
 FOR WHICH RESULTS ARE TO BE OUTPUT- IZSCAN NON-ZERO FOR Z-SCAN/PAGE
 ONE SET OF 6 PER LINE, END WITH ALL ZEROS
 : +       2   2     2   2     1  52     1
 :
 MEDIUM                  AE        AP
 FE                    0.521     0.010
 H2O521                0.521     0.010
```

NCASE, IWATCH, TIMMAX, INSEED1, INSEED2

: + 1000 0 0.99 0 0

==

Now for the Source data :

Number of Sources = 49

ID#	ENERGY	INTENSITY	CHARGE
1	0.028	405.000	-1
2	0.085	454.000	-1
3	0.142	486.000	-1
4	0.199	502.000	-1
5	0.256	504.000	-1
6	0.313	497.000	-1
7	0.370	482.000	-1
8	0.427	456.000	-1
9	0.484	423.000	-1
10	0.541	384.000	-1
11	0.598	343.000	-1
12	0.655	305.000	-1
13	0.712	273.000	-1
14	0.769	249.000	-1
15	0.826	228.000	-1
16	0.883	208.000	-1
17	0.940	193.000	-1
18	0.997	185.000	-1
19	1.054	184.000	-1
20	1.111	186.000	-1
21	1.168	186.000	-1
22	1.225	186.000	-1
23	1.282	185.000	-1
24	1.339	183.000	-1
25	1.396	180.000	-1
26	1.453	176.000	-1
27	1.510	172.000	-1
28	1.567	166.000	-1
29	1.624	160.000	-1
30	1.681	154.000	-1
31	1.738	146.000	-1
32	1.795	138.000	-1
33	1.852	130.000	-1
34	1.909	121.000	-1
35	1.966	112.000	-1
36	2.023	102.000	-1
37	2.079	93.000	-1
38	2.136	83.000	-1
39	2.193	73.000	-1
40	2.250	64.000	-1
41	2.307	54.000	-1
42	2.364	45.000	-1
43	2.421	37.000	-1
44	2.478	29.000	-1
45	2.535	21.000	-1
46	2.592	15.000	-1
47	2.649	9.000	-1
48	2.706	5.000	-1
49	2.763	2.000	-1

The number of source [illegible]ions = 49

SREG#	X LOW	X UP[illegible]	Y LOW	Y UPP	Z LOW	Z UPP	RHO	ID
1	0.000	12.[illegible]	0.000	12.000	0.000	0.500	1.00	1
2	0.000	12.000	0.000	12.000	0.000	0.500	1.00	2
3	0.000	12.000	0.000	12.000	0.000	0.500	1.00	3
4	0.000	12.000	0.000	12.000	0.000	0.500	1.00	4
5	0.000	12.000	0.000	12.000	0.000	0.500	1.00	5
6	0.000	12.000	0.000	12.000	0.000	0.500	1.00	6

7	0.000	12.000	0.000	12.000	0.000	0.500	1.00	7
8	0.000	12.000	0.000	12.000	0.000	0.500	1.00	8
9	0.000	12.000	0.000	12.000	0.000	0.500	1.00	9
10	0.000	12.000	0.000	12.000	0.000	0.500	1.00	10
11	0.000	12.000	0.000	12.000	0.000	0.500	1.00	11
12	0.000	12.000	0.000	12.000	0.000	0.500	1.00	12
13	0.000	12.000	0.000	12.000	0.000	0.500	1.00	13
14	0.000	12.000	0.000	12.000	0.000	0.500	1.00	14
15	0.000	12.000	0.000	12.000	0.000	0.500	1.00	15
16	0.000	12.000	0.000	12.000	0.000	0.500	1.00	16
17	0.000	12.000	0.000	12.000	0.000	0.500	1.00	17
18	0.000	12.000	0.000	12.000	0.000	0.500	1.00	18
19	0.000	12.000	0.000	12.000	0.000	0.500	1.00	19
20	0.000	12.000	0.000	12.000	0.000	0.500	1.00	20
21	0.000	12.000	0.000	12.000	0.000	0.500	1.00	21
22	0.000	12.000	0.000	12.000	0.000	0.500	1.00	22
23	0.000	12.000	0.000	12.000	0.000	0.500	1.00	23
24	0.000	12.000	0.000	12.000	0.000	0.500	1.00	24
25	0.000	12.000	0.000	12.000	0.000	0.500	1.00	25
26	0.000	12.000	0.000	12.000	0.000	0.500	1.00	26
27	0.000	12.000	0.000	12.000	0.000	0.500	1.00	27
28	0.000	12.000	0.000	12.000	0.000	0.500	1.00	28
29	0.000	12.000	0.000	12.000	0.000	0.500	1.00	29
30	0.000	12.000	0.000	12.000	0.000	0.500	1.00	30
31	0.000	12.000	0.000	12.000	0.000	0.500	1.00	31
32	0.000	12.000	0.000	12.000	0.000	0.500	1.00	32
33	0.000	12.000	0.000	12.000	0.000	0.500	1.00	33
34	0.000	12.000	0.000	12.000	0.000	0.500	1.00	34
35	0.000	12.000	0.000	12.000	0.000	0.500	1.00	35
36	0.000	12.000	0.000	12.000	0.000	0.500	1.00	36
37	0.000	12.000	0.000	12.000	0.000	0.500	1.00	37
38	0.000	12.000	0.000	12.000	0.000	0.500	1.00	38
39	0.000	12.000	0.000	12.000	0.000	0.500	1.00	39
40	0.000	12.000	0.000	12.000	0.000	0.500	1.00	40
41	0.000	12.000	0.000	12.000	0.000	0.500	1.00	41
42	0.000	12.000	0.000	12.000	0.000	0.500	1.00	42
43	0.000	12.000	0.000	12.000	0.000	0.500	1.00	43
44	0.000	12.000	0.000	12.000	0.000	0.500	1.00	44
45	0.000	12.000	0.000	12.000	0.000	0.500	1.00	45
46	0.000	12.000	0.000	12.000	0.000	0.500	1.00	46
47	0.000	12.000	0.000	12.000	0.000	0.500	1.00	47
48	0.000	12.000	0.000	12.000	0.000	0.500	1.00	48
49	0.000	12.000	0.000	12.000	0.000	0.500	1.00	49

End of the Source data :

```
================================================================
 Reg:    1 Bnds(XYZ)=(    0.000   12.000)(    0.000   12.000)(    0.000     0.500)
CPUTIME SO FAR=          8.380 s

 Reg:    2 Bnds(XYZ)=(    0.000   12.000)(    0.000   12.000)(    0.000     0.500)
CPUTIME SO FAR=         31.940 s

 Reg:    3 Bnds(XYZ)=(    0.000   12.000)(    0.000   12.000)(    0.000     0.500)
CPUTIME SO FAR=         79.640 s

 Reg:    4 Bnds(XYZ)=(    0.000   12.000)(    0.000   12.000)(    0.000     0.500)
CPUTIME SO FAR=        141.130 s

 Reg:    5 Bnds(XYZ)=(    0.000   12.000)(    0.000   12.000)(    0.000     0.500)
CPUTIME SO FAR=        214.040 s

 Reg:    6 Bnds(XYZ)=(    0.000   12.000)(    0.000   12.000)(    0.000     0.500)
CPUTIME SO FAR=        296.770 s

 Reg:    7 Bnds(XYZ)=(    0.000   12.000)(    0.000   12.000)(    0.000     0.500)
CPUTIME SO FAR=        388.450 s
```

```
 Reg:  30 Bnds(XYZ)=(    0.000   12.000)(    0.000   12.000)(    0.000    0.500)
CPUTIME SO FAR=     4725.650 s

 Reg:  31 Bnds(XYZ)=(    0.000   12.000)(    0.000   12.000)(    0.000    0.500)
CPUTIME SO FAR=     5000.520 s

 Reg:  32 Bnds(XYZ)=(    0.000   12.000)(    0.000   12.000)(    0.000    0.500)
CPUTIME SO FAR=     5284.130 s

 Reg:  33 Bnds(XYZ)=(    0.000   12.000)(    0.000   12.000)(    0.000    0.500)
CPUTIME SO FAR=     5573.400 s

 Reg:  34 Bnds(XYZ)=(    0.000   12.000)(    0.000   12.000)(    0.000    0.500)
CPUTIME SO FAR=     5873.300 s

 Reg:  35 Bnds(XYZ)=(    0.000   12.000)(    0.000   12.000)(    0.000    0.500)
CPUTIME SO FAR=     6178.250 s

 Reg:  36 Bnds(XYZ)=(    0.000   12.000)(    0.000   12.000)(    0.000    0.500)
CPUTIME SO FAR=     6486.600 s

 Reg:  37 Bnds(XYZ)=(    0.000   12.000)(    0.000   12.000)(    0.000    0.500)
CPUTIME SO FAR=     6800.400 s

 Reg:  38 Bnds(XYZ)=(    0.000   12.000)(    0.000   12.000)(    0.000    0.500)
CPUTIME SO FAR=     7130.080 s

 Reg:  39 Bnds(XYZ)=(    0.000   12.000)(    0.000   12.000)(    0.000    0.500)
CPUTIME SO FAR=     7458.410 s

 Reg:  40 Bnds(XYZ)=(    0.000   12.000)(    0.000   12.000)(    0.000    0.500)
CPUTIME SO FAR=     7798.110 s

 Reg:  41 Bnds(XYZ)=(    0.000   12.000)(    0.000   12.000)(    0.000    0.500)
CPUTIME SO FAR=     8144.020 s

 Reg:  42 Bnds(XYZ)=(    0.000   12.000)(    0.000   12.000)(    0.000    0.500)
CPUTIME SO FAR=     8499.689 s

 Reg:  43 Bnds(XYZ)=(    0.000   12.000)(    0.000   12.000)(    0.000    0.500)
CPUTIME SO FAR=     8859.131 s

 Reg:  44 Bnds(XYZ)=(    0.000   12.000)(    0.000   12.000)(    0.000    0.500)
CPUTIME SO FAR=     9228.939 s

 Reg:  45 Bnds(XYZ)=(    0.000   12.000)(    0.000   12.000)(    0.000    0.500)
CPUTIME SO FAR=     9598.320 s

 Reg:  46 Bnds(XYZ)=(    0.000   12.000)(    0.000   12.000)(    0.000    0.500)
CPUTIME SO FAR=     9967.270 s

 Reg:  47 Bnds(XYZ)=(    0.000   12.000)(    0.000   12.000)(    0.000    0.500)
CPUTIME SO FAR=    10352.180 s

 Reg:  48 Bnds(XYZ)=(    0.000   12.000)(    0.000   12.000)(    0.000    0.500)
CPUTIME SO FAR=    10743.280 s

 Reg:  49 Bnds(XYZ)=(    0.000   12.000)(    0.000   12.000)(    0.000    0.500)
CPUTIME SO FAR=    11136.439 s

0TOTAL CPUTIME FOR SIMULATIONS=       402.7 s  =      0.112 hr

TOTAL ENERGY DEPOSITED IN VOLUME per DECAY =  0.8073E+00 ✓
```

just under $\bar{T}_0$ for betas. Not exactly $\bar{T}_0$ because some β's [crosses?] the phantom

```
1          The dose to big cube of water perfused with a Mn-56 source spectrum
           XYZ(V01) DOSE OUTPUTS   Gy/ Disintegration

                FOR X=      2.000 TO     10.000      I=  2
 OYBOUNDS:  2.000       10.000
          J=          2
  ZBOUNDS (       0.000)
    0.100    1  2.089E-13- 1.4%
    0.200    2  2.329E-13- 2.2%
    0.300    3  2.292E-13- 1.8%
    0.400    4  2.397E-13- 1.7%
    0.410    5  2.292E-13- 3.2%

    0.420    6  2.336E-13- 3.9%
    0.430    7  2.207E-13- 2.4%
    0.440    8  2.262E-13- 4.6%
    0.450    9  2.181E-13- 3.5%
    0.460   10  2.130E-13- 3.5%

    0.470   11  2.179E-13- 4.4%
    0.480   12  2.005E-13- 3.6%
    0.490   13  1.842E-13- 3.5%
    0.500   14  1.417E-13- 3.5%
    0.510   15  1.190E-13- 6.3%

    0.520   16  1.119E-13- 7.1%
    0.530   17  1.017E-13- 5.6%
    0.540   18  9.545E-14- 6.4%
    0.550   19  8.945E-14- 5.6%
    0.560   20  8.297E-14- 7.7%

    0.570   21  7.429E-14- 4.2%
    0.580   22  6.767E-14- 7.4%
    0.590   23  6.458E-14- 6.9%
    0.600   24  6.284E-14- 7.1%
    0.610   25  5.662E-14- 8.9%

    0.620   26  5.750E-14- 7.2%
    0.630   27  5.258E-14- 8.3%
    0.640   28  5.470E-14- 7.3%
    0.650   29  4.939E-14- 7.6%
    0.660   30  4.703E-14- 8.2%

    0.670   31  4.712E-14- 7.7%
    0.680   32  4.263E-14- 8.7%
    0.690   33  4.217E-14- 7.3%
    0.700   34  4.114E-14- 6.9%
    0.800   35  2.998E-14- 5.8%

    0.900   36  1.833E-14- 9.7%
    1.000   37  9.706E-15-15.3%
    1.100   38  4.820E-15-12.0%
    1.200   39  1.730E-15-22.7%
    1.300   40  7.569E-16-26.0%

    1.400   41  4.322E-16-30.5%
    1.500   42  1.410E-16-40.1%
    1.600   43  6.851E-17-64.2%
    1.700   44  4.368E-17-81.8%
    1.800   45  8.024E-17-58.8%

    1.900   46  1.786E-1 -57.1%
    2.000   47  7.528E-17-73.6%
```

2.100	48	3.085E-16-56.0%
2.200	49	2.475E-16-61.2%
2.300	50	1.00[illegible]E-16-96.4%
2.400	51	1.452E-16-85.0%
2.500	52	1.463E-17-99.9%

Int. J. Radiation Oncology Biol. Phys. Vol. 19, pp. 1027–1035

● *Technical Innovations and Notes*

MONTE CARLO AND CONVOLUTION DOSIMETRY FOR STEREOTACTIC RADIOSURGERY

SHRIKANT S. KUBSAD, M.S., T. ROCKWELL MACKIE, PH.D., MARK A. GEHRING, B.S., DAVID J. MISISCO, M.S., BHUDATT R. PALIWAL, PH.D., MINESH P. MEHTA, M.D. AND TIMOTHY J. KINSELLA, M.D.

Departments of Human Oncology and Medical Physics, University of Wisconsin Medical School, Madison, WI 53792 USA

The dosimetry of small photon beams used for stereotactic radiosurgery was investigated using Monte Carlo simulation, convolution calculations, and measurements. A Monte Carlo code was used to simulate radiation transport through a linear accelerator to produce and score energy spectrum and angular distribution of 6 MV bremsstrahlung photons exiting from the accelerator treatment head. These photons were then transported through a stereotactic collimator system and into a water phantom placed at isocenter. The energy spectrum was also used as input for the convolution method of photon dose calculation. Monte Carlo and convolution results were compared with the measured data obtained using an ionization chamber, a diode, and film.

Monte Carlo, Convolution, Small beam photon dosimetry, Stereotactic radiosurgery.

INTRODUCTION

Stereotactic external beam radiosurgery was initiated by Leksell in Sweden in 1951 (15, 16). Since then, radiosurgery has been performed with X rays, protons, heavy charged particles, and gamma rays. The method involves delivery of a high radiation dose in a single fraction to a small intracranial target. Leksell's work led to the development of the commercially available Gamma Knife unit which consists of 201 ^{60}Co γ-ray sources. The Gamma Knife has been widely used to treat arteriovenous malformations and brain neoplasms. Using a proton beam, Kjellberg *et al.* have treated and followed several patients with arteriovenous malformations and have analyzed the post-treatment cure and complications (11, 12). They also established a correlation between dose and beam diameter to predict post-treatment complications.

Recent developments have led to the conversion of linear accelerators into stereotactic tools. The use of a linear accelerator for radiosurgery is gaining popularity over the Gamma Knife mainly because linear accelerators are available in most medical centers practicing conventional radiation therapy and are cost-effective. The use of a linear accelerator for stereotactic radiosurgery and its advantages over other approaches have been discussed elsewhere (3, 8, 9, 10, 17, 26, 31). Since stereotactic radiosurgery delivers high doses of radiation in a single fraction to a small target volume (the radiation field sizes are typically from 0.5 cm to 4.0 cm in diameter), accurate dosimetry and treatment planning are critical to the adaption of a linear accelerator for radiosurgery.

There are two principal concerns in the dosimetry of small beams: the presence of lateral electronic disequilibrium and steep dose profiles. Ion chambers cannot predict with sufficient resolution the dose in the penumbra which, for the smallest field sizes, extends to the central axis of the field. Radiographic film and diode can provide better spatial resolution but the film has a response which varies with photon energy more than that of an ion chamber and a well shielded diode. The energy response effect could be significant in broad beam photon dosimetry because of the variation in the photon energy from the central axis to the edge of the field. This variation in the photon energy across the field is caused by the flattening filter

Presented at the 31st Annual ASTRO Meeting, 5 October 1989, San Francisco, CA.

Reprint requests to: Shrikant S. Kubsad, M.S., Department of Human Oncology, K4/B100 Clinical Science Center, 600 Highland Ave., Madison, WI 53792 USA.

Acknowledgements—The authors wish to thank Terry Cummings of Varian Associates for providing the design specifications of the Clinac-2500 linear accelerator treatment head. Paul Reckwerdt for his help in computations, Wonho Sohn for his assistance in measurements, and Drs. David W. O. Rogers and Alex F. Bielajew for their valuable discussions on Monte Carlo methods. The first author is also grateful to Drs. Claudio H. Sibata and Paul M. DeLuca, Jr., who introduced him to the Monte Carlo methods. This work was partially supported by NCI grant R29 CA48902.

Accepted for publication 26 April 1990.

which hardens the photon beam more in the central part of the beam than in the peripheral region (22). However, in a small beam the photon energy variation across the beam diameter can be negligible.

The Monte Carlo and convolution methods can be used to produce relative dose distributions free of energy response artifacts and equivalent to the resolution of diodes and film isodensitometers (1 to 2 mm), but in order to do this, information such as the energy and angular spectrum of the incident photon beam is required. The Monte Carlo method is used to produce such information and to verify the accuracy of the film and diode measurements.

METHODS AND MATERIALS

Monte Carlo method

We used the Electron Gamma Shower Version 4 (EGS4) (23) Monte Carlo code system to characterize the photon beam emerging from the accelerator treatment head. The energy spectrum of photons was used to produce a dose kernel for the stereotactic beam from monoenergetic photon beam kernels generated in water (19). The EGS4 Monte Carlo code is a general purpose coupled charged-particle-photon transport simulation system that can transport these particles in the energy range of a few keV to GeV in heterogeneous media of arbitrary 3-dimensional complex geometry (23). Many authors have demonstrated that very complex and sophisticated simulations can be done using Monte Carlo methods code (5, 8, 13, 14, 22, 24, 25, 27, 29, 30).

We developed the user main program and geometry packages to simulate the linear accelerator* treatment head (LATH), the stereotactic collimating system (SCS) and a semiinfinite water phantom placed at the isocenter (source-to-isocenter distance was 100 cm). The user main program drives the geometry package and the EGS4 Monte Carlo code to simulate particle transport using interaction probability distribution data generated by PEGS4 (Preprocessor for EGS4) (23). The user code sets in motion photon histories (simulated photons) and transports them until they are absorbed or scattered. The energy and direction of charged particles set in motion and scattered photons are determined by the EGS4 code system and subsequently transported as well. Charged particles are transported in discrete steps during which the particle is assumed to travel a straight line; however, the energy loss is scaled to account for increased pathlength caused by scattering. The user code handles the scoring (tabulation of results for a history) of one or any combination of type of particle, energy, position, and direction cosines for photons and charged particles each time a particle interaction or boundary crossing occurs. Scoring also occurs following each charged particle step. The code follows each particle and its progeny until it escapes or its energy falls below a cut-off energy set by the user to terminate the transport of that particle and deposit its remaining energy on the spot.

The schematics of a typical LATH geometry are shown in Figure 1a, whereas Figure 1b illustrates the simulated LATH geometry used in Monte Carlo method. The dimensions and distances of the LATH were obtained from the vendor and were verified during a major servicing of the machine. The primary, secondary, and stereotactic collimators and moving jaws were simulated using concentric cylindrical slabs. The thickness and radius of each slab were carefully chosen to have the same surface area as the actual LATH and to reproduce the divergence of the radiation beam. The simulation used a series of cylindrical slabs stacked on one another to match closely the profile of the flattening filter. We simulated both the upper and lower moving jaws at the same level. The stereotactic collimators were lead-filled cylinders of 15 cm in height with diverging circular holes of 0.5 cm to 4.0 cm in diameter, and were attached to the linear accelerator head.

The SCS and stereotactic base frame that mounts on the accelerator couch base plate and other quality control accessories[†] were built to specifications for our linear accelerator.* We also designed and built a stereotactic

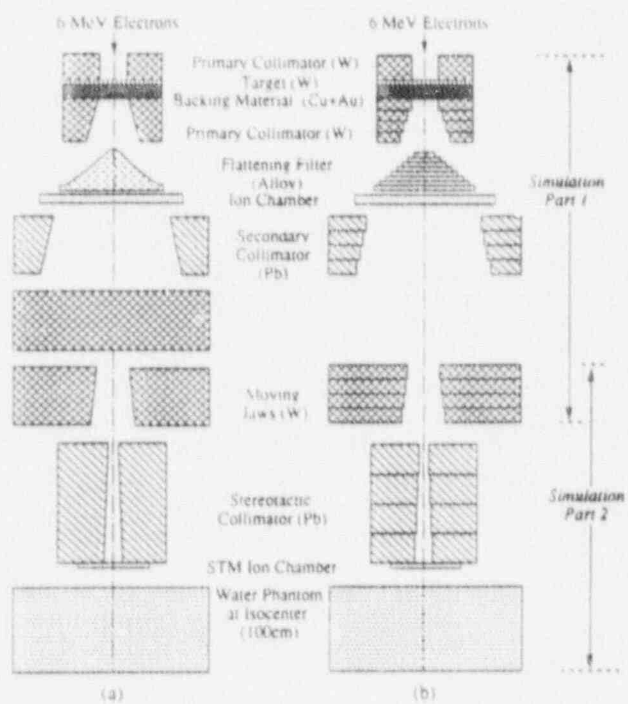

Fig. 1. (a) Schematics of the linear accelerator treatment head. (b) Simulated linear accelerator treatment head geometry used in Monte Carlo calculations.

---

* Clinac-2500, Varian Associates, Palo Alto, CA.

[†] Physical Science Laboratory, University of Wisconsin, Madison, WI.

...meters used by EGS4 in Monte Carlo simulations

...y	ECUT = 0.521 MeV
...ff	PCUT = 0.010 MeV
	ESTEPE = 1% of the electron energy at the beginning of a step
	SMAX = Smallest dimension of ROI
	NCASES = 2×10^6/ Simulation

...r (STM) air ion chamber which was ...o monitor the radiation output. This ...sed to verify the dose delivery to the

...lation was carried out in two parts. ...mulated the accelerator head from ...m of the moving jaws to score the ...aracteristics (energy spectrum and ...n a plane perpendicular to the cen-... characteristics were stored for later ...part of the simulation starts from ...he moving jaws, through the SCS, ...antom at the isocenter.

...ulation of the LATH. As depicted ...tic electrons with a kinetic energy ... the vacuum window of the ac-...ungsten target producing brems-...beam passes through the backing ... and gold alloy for fast heat dis-sipation. The beam is collimated by a primary diverging collimator made of tungsten. The flattening filter is comprised of an alloy containing steel and other elements. In addition to making the fluence distribution more uniform, the flattening filter also produces low energy electrons and photons. The beam passes through a transmission monitor chamber and is subsequently shaped by secondary lead collimators and moving tungsten jaws.

We scored the energy spectrum and angular distribution of 6 MV bremsstrahlung photons in annular regions of 1, 2, 3, and 4 cm in radius in a plane perpendicular to the central axis at 50 cm from the target. The photon energy bin width of 0.25 MeV was chosen to score the energy spectrum. For each region of interest (ROI), the photon mean planar fluence, the mean fluence, the mean energy, the fluence weighted, and the energy-fluence weighted mean energy, and the photon mean angle of incidence on the scoring plane with respect to the central axis, were calculated in each energy bin.

Simulation part 2: simulation of the SCS and water phantom. The stored spectrum was used to choose the initial energy and direction of photons transported from the bottom of the moving jaws through the SCS and in a cylindrical water phantom placed at the isocenter (the source-to-surface distance of the phantom was 100 cm). The moving jaws were included in the second part of the simulation to account for potential scatter from the bottom of the jaws and also to maintain the continuity between the two parts of the simulation. In each of the regions, the mean energy deposition, the photon mean fluence, the photon mean energy, and the photon mean incident angle with respect to the central axis were calculated. The maximum dimension of the scoring region was 0.2 cm in any direction to ensure better resolution, especially for beam profiles in a water phantom.

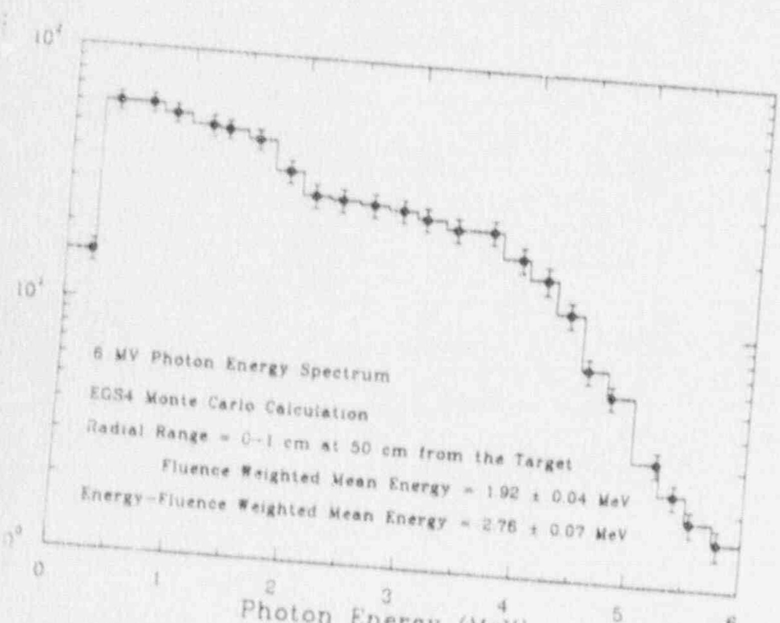

...pectrum of 6 MV photons from the linear accelerator at 50 cm from the target.

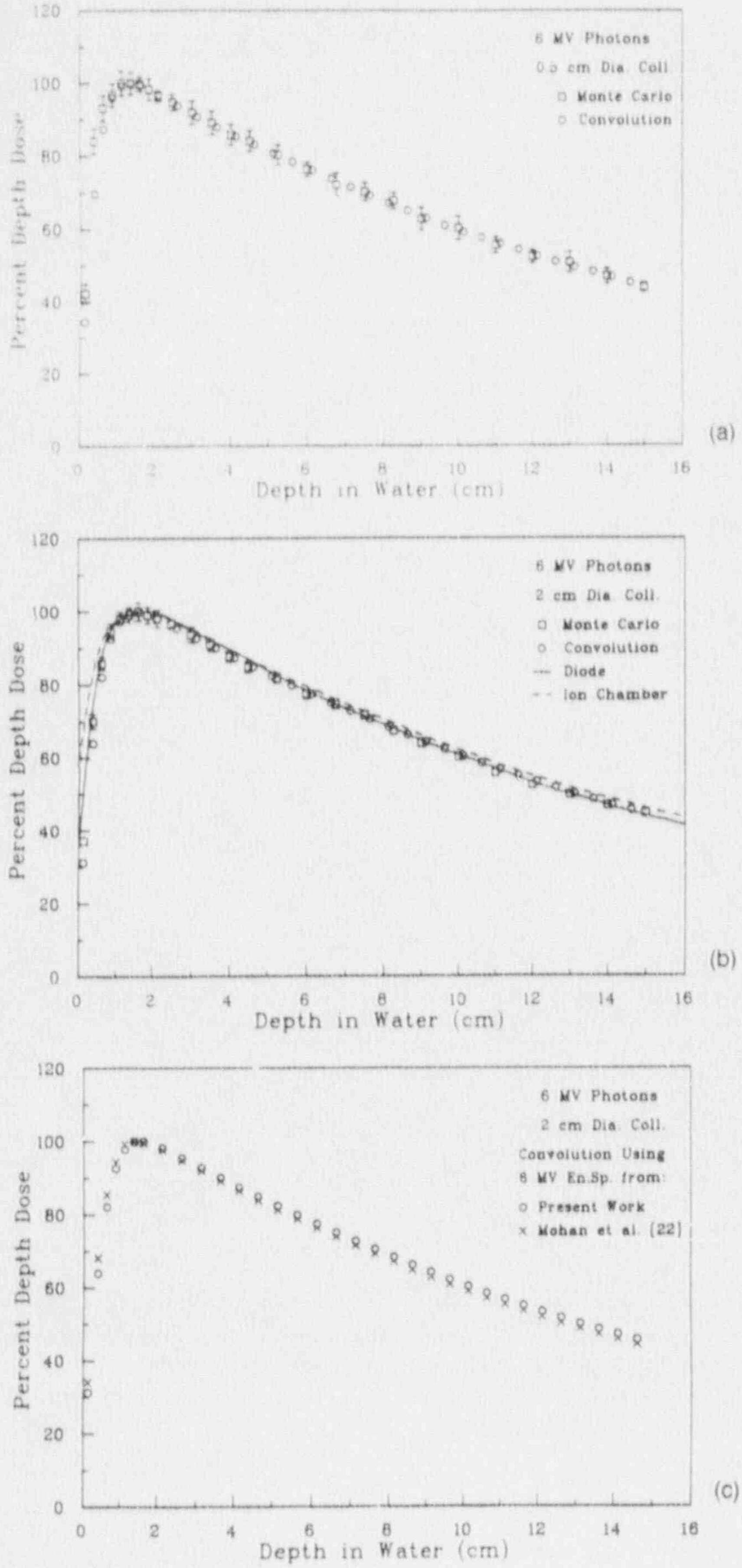

6 MV Photons
0.5 cm Dia. Coll.
Monte Carlo
Convolution
Percent Depth Dose
Depth in Water (cm)
(a)
6 MV Photons
2 cm Dia. Coll.
Monte Carlo
Convolution
Diode
Ion Chamber
Percent Depth Dose
Depth in Water (cm)
(b)
6 MV Photons
2 cm Dia. Coll.
Convolution Using
6 MV En.Sp. from:
Present Work
Mohan et al. [22]
Percent Depth Dose
Depth in Water (cm)
(c)

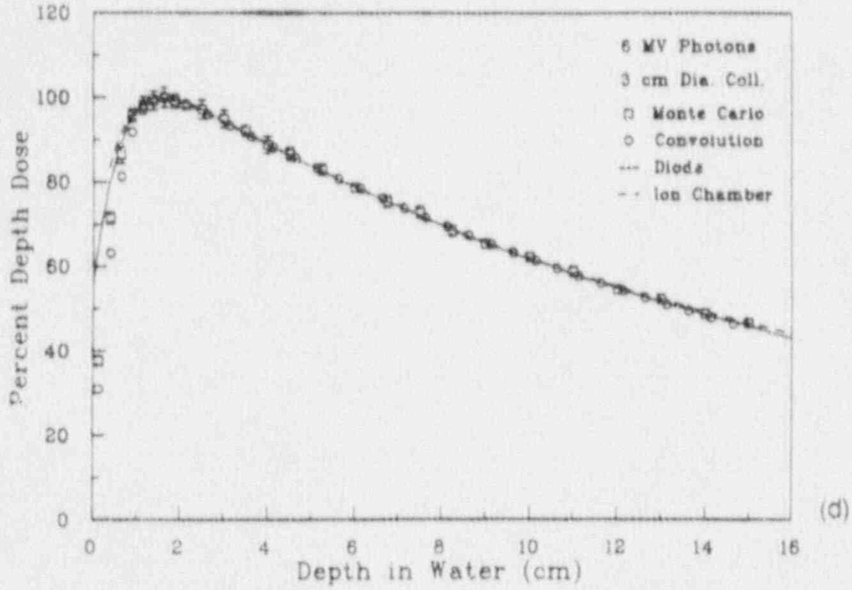

Fig. 3. (a) Central axis depth dose in water for 0.5 cm beam diameter. (b) Central axis depth dose in water for 2 cm beam diameter. (c) Central axis depth dose in water for 2 cm beam diameter. (d) Central axis depth dose in water for 3 cm beam diameter.

EGS4 transport and calculation parameters. The results of Monte Carlo simulations are very sensitive to transport parameters such as the maximum relative energy lost in an electron step (called ESTEPE in EGS4), the maximum electron step length (SMAX), the electron cutoff energy (ECUT), and the photon cutoff energy (PCUT) (4, 5, 14, 27, 28, 29). Additionally, the total number of histories transported per simulation (NCASES) dictates the accuracy of the final results. Moreover, the random sampling of incident particle's energy, position and direction cosines at the beginning of simulation directly affect the final outcome. The secondary electron production energy threshold (AE) of 0.521 MeV and secondary photon production energy threshold (AP) of 0.01 MeV were used by the PEGS4 to generate the interaction probability distribution data for electron and photon transport. The EGS4 used the data produced by the PEGS4 and also used the transport parameters shown in Table 1 to carry out the simulations.

The particles were terminated when their energy fell below the cut-off energy or escaped the simulation geometry. When particle termination occurred, the residual kinetic energy of the particle was deposited locally.

Each simulation of 2 million histories was divided into 10 batches for statistical analysis. The standard error in each scored quantity was determined from a calculation of one standard deviation from the 10 batches.

Convolution method

A number of authors have shown that the convolution of a primary intensity function and a spatially invariant kernel models the dose distribution well in a homogeneous phantom (1, 2, 7, 18, 19, 20, 21). The primary intensity function models the primary photon transport up to and inside the phantom and the kernel accounts for secondary particle transport in the phantom.

The dose distribution $D(\vec{r})$ in a homogeneous phantom can be given by the equation:

$$D(\vec{r}) = \int \frac{\mu}{\rho}(\vec{r}')\Psi(\vec{r}')A(\vec{r} - \vec{r}')d^3r' \qquad (1)$$

where $(\mu/\rho)(\vec{r}')$ is the appropriate mass attenuation coefficient distribution, $\Psi(\vec{r}')$ is the energy fluence distribution, and $A(\vec{r} - \vec{r}')$ is the convolution kernel.

The details of the convolution/superposition software have been described elsewhere (20). The superposition method involves modifying the convolution kernel to take into account transport through heterogeneous phantoms; however, this capability was not required in this study because the phantom was homogeneous. The voxels were solid rectangles (i.e., the voxel dimensions may vary in each direction). The voxel thickness was 0.25 cm in all of the calculations and the voxel areas were 0.1×0.1 cm^2 for the 0.5 cm and 1.0 cm collimators and 0.2×0.2 cm^2 for the larger collimators.

Most of the convolution/superposition software is concerned with modelling the primary energy fluence distribution. The software is capable of modeling the "horns" in the incident energy fluence distribution, spectral hardening in the depth direction, and "softening" in the lateral direction mainly because of a reduced thickness of primary rays that have travelled through the field flattening filter. The beam is first modelled as diverging from a point source and exiting through a perfect circular aperture with constant energy fluence across the field. The energy flu-

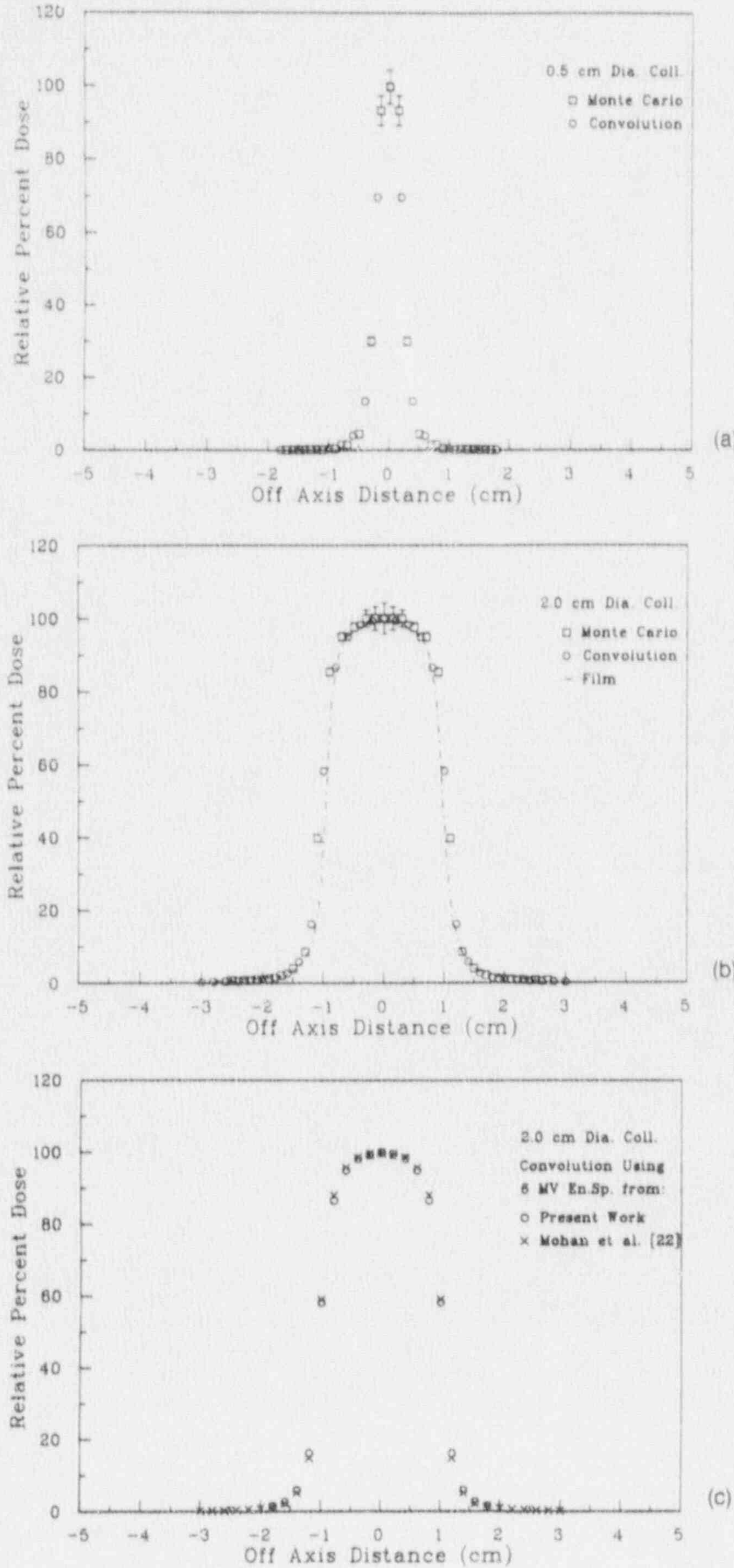

0.5 cm Dia. Coll.
□ Monte Carlo
○ Convolution
Relative Percent Dose
Off Axis Distance (cm)
(a)
2.0 cm Dia. Coll.
□ Monte Carlo
○ Convolution
-- Film
Relative Percent Dose
Off Axis Distance (cm)
(b)
2.0 cm Dia. Coll.
Convolution Using
6 MV En.Sp. from:
○ Present Work
× Mohan et al. [22]
Relative Percent Dose
Off Axis Distance (cm)
(c)

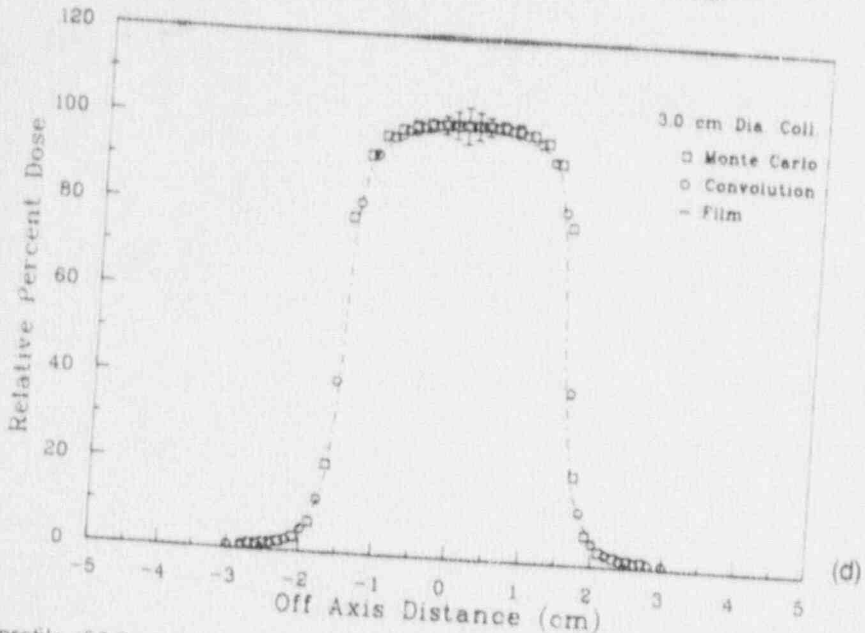

4. (a) Beam profile of 0.5 cm beam diameter at 5 cm depth in water. (b) Beam profile of 2 cm beam diameter cm depth in water. (c) Beam profile of 2 cm beam diameter at 5 cm depth in water. (d) Beam profile of 3 cm n diameter at 5 cm depth in water.

ımed to decrease exponentially (with distance ıe phantom and with an inverse-square fall- surface.

:n by the following equation:

$$\Psi = \Psi_0 e^{-\mu_{eff} d}\left(\frac{SSD}{SSD + d}\right)^2 \quad (2)$$

e surface energy fluence, μ_{eff} is the effective efficient, and SSD is the source-to-surface

attenuation coefficient was obtained from coefficients weighted with respect to the of the spectrum. We used the spectrum is work (illustrated in Fig. 2) and a pub- from Mohan *et al.* (22). The effective n coefficient at the surface of the phantom /g and 0.0481 cm²/g for those spectra.

l model of energy fluence was modified r for primary energy fluence outside the ıe beam boundary. The primary fluence consists of several components: trans- he collimators, photons scattered outside the accelerator structure, and the colli- cal penumbra due to a finite source size. imary" energy fluence should be quali- photon energy fluence which has not the phantom regardless of its origin in pical values of the primary fluence out-

side a field in routine external beam radiotherapy are from 3 to 5% from the first two of the above components. However, it was found that the secondary stereotactic collimators effectively reduced this component of the fluence to zero (±0.1%). The geometrical penumbra can be accounted for using a modification of a procedure proposed by Boyer (6). It involves specifying an effective source size (s_{eff}, taken to be 0.2 cm) and the source-to-collimator distance (SCD) of 77 cm, which is the distance from the source to the end of the stereotactic collimator. The model assumes that a finite source size can be modelled as a convolution of the energy fluence with a 2-D Gaussian distribution with a width (FWHM) at a source-to-point distance (SPD) equal to the following:

$$FWHM = s_{eff}\frac{SPD}{SCD} \quad (3)$$

The finite voxel size introduces a blurring artifact (analogous to the finite size of a detector) that mimics a finite source size in its effects. Therefore, FWHM is reduced by an amount equal to the lateral voxel dimension (i.e., either 0.1 cm or 0.2 cm).

Measurements

We used a small diode and a small ionization chamber* with a three-dimensional scanner in a water phantom to acquire depth doses and beam profiles.[†] Film dosimetric measurements were carried out by exposing radiographic verification films[‡] in a Solid Water Phatom.[§] The films

Kallered, Sweden.
ıeTek OY, Espoo, Finland, driven by HP lett-Packard Co., Fort Collins, CO.

[‡] Kodak X-Omat V, Eastman Kodak Company, Rochester, NY.
[§] Radiation Measurements Inc., Madison WI.

were processed using a rapid processor.** A film scanning densitometer,†† driven by a stepper-motor controller board‡‡ in a PC§§ and controlled by software written using a data acquisition package,*** was used to scan the processed films to acquire depth doses and beam profiles. The diameter of the isodensitometer light spot was 1.0 ± 0.2 mm.

RESULTS

Energy spectrum and angular distribution

The energy spectrum of 6 MV bremsstrahlung photons from the linear accelerator is shown in Figure 2. At 50 cm from the target, the fluence and energy-fluence weighted photon energies at the central axis (within radial range between 0 to 1 cm) were 1.92 ± 0.04 and 2.76 ± 0.07 MeV, respectively. The fluence and energy-fluence weighted photon mean incident angles with respect to the central axis were 1.61 ± 0.08 and 1.21 ± 0.05 degrees, respectively.

Central axis relative depth doses in water

The relative percent depth doses in water for beam diameters of 0.5, 1, 2, 3, and 4 cm were computed using direct Monte Carlo simulation and convolution calculations using photon spectrum from the present work and a published spectrum (22). Comparisons with the measured data for beam diameters of 0.5, 2, and 3 cm are shown in Figure 3. There is excellent agreement between the results of Monte Carlo, convolution calculations, and diode measurements beyond the depth of peak dose. Within the build up region for 2 and 3 cm beam diameters, the results of Monte Carlo and convolution calculations agree with the diode measurements within 2% and 5%, respectively. The depth doses for beam diameters of 0.5 to 4 cm, derived by Monte Carlo and convolution methods, are in excellent agreement beyond the depth of peak dose, but in the build up region a disagreement of 2 to 10% is observed. This may be because the low energy scattered photons and electrons arising from the SCS are not accounted for in the convolution calculations. The depth doses derived by convolution method using the photon spectrum produced in this work and the published spectrum from Mohan *et al.* (22) agree within 3%. The measured depth dose by diode and depth ionization by ion chamber measurements are in good agreement for large beam diameter (≥3 cm) as shown in Figure 3d, whereas increased disagreement is observed as the beam diameter is decreased. This could be because of the larger size of the ion chamber in a small radiation beam. The depth of peak dose for 0.5 to 4 cm beam diameters ranged from 1.38 to 1.75 cm. The decrease in the depth of peak dose for smaller field sizes is caused by decreased lateral scatter contribution to the depth dose.

Relative beam profiles in water

The relative beam profiles at a depth of 5 cm in water for beam diameters of 0.5, 1, 2, 3, and 4 cm were computed using direct Monte Carlo and convolution calculations using photon spectrum from the present work and the published spectrum (22). Comparisons of the calculated and measured data for beam diameters of 0.5, 2, and 3 cm are shown Figure 4. Again, there is excellent agreement between the profiles obtained by Monte Carlo and convolution calculations, and film dosimetry. The disagreement between Monte Carlo and convolution results in the beam boundary region can be reduced if the size of the scoring regions are further decreased below 0.2 cm in the radial direction in calculational methods but at the expense of increased computing time for Monte Carlo calculation. There is excellent agreement outside the primary beam because appropriate penumbral corrections have been employed in the convolution calculations. Note that the uncertainty has decreased radially outward because the volume of scoring regions (volume = $\pi r^2 h$) increases as a function of radius to the power two, thereby resulting in a larger number of histories in those regions.

Computation times

We used a workstation* (≃5 times faster than a mini computer†) to perform simulations. Monte Carlo calculation used 120 CPU hours to transport 2 million initial electron histories through the linear accelerator head to obtain the photon energy spectrum and other characteristics, whereas the same number of initial photon spectral histories transported in water to obtain depth doses and beam profiles required an average of 80 CPU hr per beam diameter. The average computing time for the convolution calculations was 0.06 CPU hr per simulation on the same system.

DISCUSSION

We have shown that the Monte Carlo method can be used to characterize the 6MV bremsstrahlung photon beam produced by the linear accelerator and to obtain the dosimetric for small radiation fields used in stereotactic radiosurgery. We found that the simulation of exact dimensions of target, backing material, and flattening filter and appropriate Monte Carlo transport parameters were

** Kodak RP-X Omat rapid processor, Eastman Kodak Company, Rochester, NY.

†† Artronix, St. Louis, MO.

‡‡ METRABYTE, Metrabyte Corporation, Taunton, MA.

§§ Leading Edge PC, Leading Edge Products Inc., Needham Heights, MA.

*** ASYST, Asyst Software Technologies Inc., Rochester, NY.

* Sun 4/110, Sun Microsystems Inc., Mountain View, CA.

† VAX 11/780, Digital Equipment Corporation, Maryland, MA.

important in acquiring accurate photon energy spectra and angular distributions. Our user-written programs can be generalized to simulate other treatment machines to obtain beam and dosimetric data. Similarly, we have shown that the convolution techniques using Monte Carlo-produced photon energy spectra can calculate dosimetric data used for stereotacic radiosurgery. The results of Monte Carlo and convolution methods are in excellent agreement with the measured data. The spatial resolution of Monte Carlo and convolution methods were adequate and comparable to film and diodes for use in small beam dosimetry.

We have developed in-house a stereotactic treatment planning system which uses the dosimetric data base generated by the convolution method. The simulation of the accelerator treatment head by the Monte Carlo method was required to obtain the energy spectra used for the convolution method and to provide a clarification of its dose predictions independent of measurements. In summary, we have demonstrated that the Monte Carlo and convolution methods are powerful and practical tools to generate accurate dosimetric data. These methods can become the basis for dose computation in the routine clinical treatment planning algorithms using fast computers.

REFERENCES

1. Ahnesjö, A. Collapsed cone convolution of radiant energy for photon dose calculation in heterogeneous media. Med. Phys. 16:577–592; 1989.
2. Ahnesjö, A.; Andreo, P.; Brahme, A. Calculation and application of point spread functions for treatment planning with high energy photon beams. Acta Oncol. 26:49–57; 1987.
3. Betti, O. O.; Munari, C.; Rosler, R. Stereotactic radiosurgery with the linear accelerator: treatment of arteriovenous malformations. Neurosurgery 24:311–321; 1989.
4. Bielajew, A. F.; Rogers, D. W. O. PRESTA—The Parameter Reduced Electron-Step Transport Algorithm for electron Monte Carlo transport. Nucl. Instr. Meth. B18:165–181; 1987.
5. Bielajew, A. F.; Rogers, D. W. O.; Nahum, A. E. The Monte Carlo simulation of ion chamber response to ^{60}Co—resolution of anomalies associated with interfaces. Phys. Med. Biol. 30:419–427; 1985.
6. Boyer, A. Fourier convolution techniques. Proceedings of the Regina Workshop on Convolution. Regina, Canada. October 16–17, 1986.
7. Boyer, A.; Mok, E. A photon dose distribution model employing convolution calculations. Med. Phys. 12:169–177; 1985.
8. Colombo, F.; Benedetti, A.; Pozza, F.; Avanzo, R. C.; Marchettic, C.; Chierego, G.; Zanardo, A. External stereotactic irradiation by linear accelerator. Neurosurgery 16:154–159; 1985.
9. Colombo, F.; Benedetti, A.; Pozza, F.; Zanardo, A.; Avanzo, R. C.; Chierego, G.; Marchetti, C. Stereotactic radiosurgery utilizing a linear accelerator. Appl. Neurophysiol. 48:133–145; 1985.
10. Hartmann, G. H.; Schlegel, W.; Strum, V.; Kober, B.; Pastyr, O.; Lorenz, W. J. Cerebral radiation surgery using moving field irradiation at a linear accelerator facility. Int. J. Radiat. Oncol. Biol. Phys. 11:1185–1192; 1985.
11. Kjellberg, R. N.; Davis, K. R.; Lyson, S.; Butler, W.; Adams, R. D. Bragg peak proton therapy for arteriovenous malformations of the brain. Clin. Neurosurgery 31:248–290; 1984.
12. Kjellberg, R. N.; Hanamura, T.; Davis, K. R.; Lyson, S.; Adams, R. D. Bragg peak proton therapy for arteriovenous malformations of the brain. N. Engl. J. Med. 309:269–274; 1983.
13. Kubsad, S. S.; Mackie, T. R.; Paliwal, B. R.; Attix, F. H. Monte Carlo calculation of electron and secondary photon spectra from a Varian Clinac-2500. Med. Phys. 16:49; 1989 (Abstr).
14. Kubsad, S. S.; Paliwal, B. R.; Sibata, C. H.; Attix, F. H. Ion chamber electron fluence corrections for electron beams (Abstr). Med. Phys. 13:605; 1986.
15. Leksell, L. Stereotaxis method and radiosurgery of the brain. Acta Chir. Scand. 102:316–319; 1951.
16. Leksell, L. Stereotactic radiosurgery. J. Neurol. Neurosurg. Physiat. 46:797–803; 1983.
17. Lutz, W.; Winston, K. R.; Maleki, N. A system for stereotactic radiosurgery with a linear accelerator. Int. J. Radiat. Oncol. Biol. Phys. 14:373–381; 1988.
18. Mackie, T. R.; Ahnesjö, A.; Dickof, P.; Snider, A. Development of convolution/superposition method for photon beams. Proceedings of IXth ICCR, International Conference on Computers in Radiation Therapy, Den Haag, The Netherlands. 1987:107–110.
19. Mackie, T. R.; Bielajew, A. F.; Rogers, D. W. O.; Battista, J. J. Generation of energy deposition kernels using the EGS Monte Carlo code. Phys. Med. Biol. 33:1–20; 1988.
20. Mackie, T. R.; Scrimger, J. W.; Battista, J. J. A convolution method of calculating dose for 15 MV x-rays. Med. Phys. 12:188–196; 1985.
21. Mohan, R.; Chui, C.; Lidofsky, L. Differential pencil beam dose computation model for photons. Med. Phys. 13:64–73; 1986.
22. Mohan, R.; Chui, C.; Lidofsky, L. Energy and angular distributions from medical linear accelerators. Med. Phys. 12:592–597; 1985.
23. Nelson, W. R.; Hirayama, H.; Rogers, D. W. O. The EGS4 Code System. Stanford Linear Accelerator Report SLAC-265; 1985.
24. Petti, P. L.; Goodman, M. S.; Gabriel, T. A.; Mohan, R. Investigation of build up dose from electron contamination of clinical photon beams. Med. Phys. 10:18–24; 1983.
25. Petti, P. L.; Goodman, M. S.; Sisterson, J. M.; Biggs, P. J.; Gabriel, T. A.; Mohan, R. Source of electron contamination for the Clinac-35 25 MV photon beam. Med. Phys. 10:856–861; 1983.
26. Rice, R. K.; Hansen, J. L.; Svensson, G. K.; Siddon, R. L. Measurements of dose distributions in small beams of 6 MV x-rays. Phys. Med. Biol. 32:1087–1099; 1987.
27. Rogers, D. W. O. Low energy electron transport with EGS. Nucl. Instr. Meth. A227:535–548; 1984.
28. Rogers, D. W. O. More realistic Monte Carlo calculations of photon detector response functions. Nucl. Instr. Meth. 199:531–548; 1982.
29. Rogers, D. W. O.; Ewart, G. M.; Bielajew, A. F. Calculation of contamination of the ^{60}Co beam from an AECL therapy source. National Research Council of Canada Report No. PXNR-2710; 1985.
30. Udale, M. A Monte Carlo investigation of surface doses for broad electron beams. Phys. Med. Biol. 33:939–954; 1988.
31. Winston, K. R.; Lutz, W. Linear accelerator as a neurosurgical tool for stereotactic radiosurgery. Neurosurgery 22:454–464; 1988.